AN ANALYSIS AND DESIGN OF A LINEAR GUARDED CUT-BAR APPARATUS FOR THERMAL CONDUCTIVITY MEASUREMENTS.

By

David A. Didion

Technical Report No. 2

Prepared Under Contract NONR 2249 (12)
for

Office of Naval Research
Washington, D. C. 20390

31 January 1968

The Catholic University of America
Department of Mechanical Engineering
Washington, D. C. 20017

ACKNOWLEDGEMENTS

It should be noted that the Analysis discussed in this report has been influenced by similar work in References [2] and [3]. Since these References are not readily available in the open literature Figure 11 and its related discussion have been included for the sake of completeness.

The author wishes to express his gratitude to Professor Michael Chi for his assistance with the mathematical analysis and Mr. L. Fisher for the programming and Figure construction.

TABLE OF CONTENTS

	Page
Abstract	iv
List of Figures	v
Nomenclature	vi
I. Introduction	1
II. Analysis	5
III. Design	13
IV. References	25
Appendices	
A. Mathematical Analysis of the Geometrical Factor	26
B. Computer Program for the Geometrical Factor	42

ABSTRACT

A quantitative analysis of the Cut-Bar method of measuring the thermal conductivity of solids is performed. The mathematical model, which corrects for the difference in heat flux in the specimen and reference standard, is that of the two dimensional steady heat conduction equation applied to an annulus of insulation. The solution is presented in detail and found to be comprised of two physically distinct parts, a conductivity factor and a geometrical factor. A number of charts and graphs are presented for clarification as to the nature and magnitude the relative sizes of the various components will have on the accuracy over different conductivity ranges. The complexity of the geometrical factor required a digital computer programs which are included.

Reference is made to a similar study, performed by researchers at the National Bureau of Standards. It is found that the differences in the guard temperature distribution results in a substantial change in the geometrical factor.

LIST OF FIGURES

Figures		Page
1.	Cut-Bar Apparatus	3
2.	Temperatures on the Boundary Surfaces of the Powder Insulation Annulus	4
3.	Shunting of Heat Flux in a Cut-Bar Apparatus	8
4.	Plot of the Geometrical Factor and Fractional Power Change	9
5.	Computer Output	10
6.	Comparison of Geometrical Factors	11
7.	Geometrical Factor as a Function of the Ratio of Apparatus Diameters	12
8.	Design Chart	18
9.	Design Chart for Optimum Dimensions	19
10.	Effect of Specimen Thermal Conductivity	20
11.	Maximum Errors for Various Ranges of Specimen Thermal Conductivity	21
12.	Plot of the Fractional Power Change	22
13.	Computer Output	23
14.	Plot of the Geometrical Factor and Fractional Power Change	24
A-1	Schematic of the Cut-Bar Apparatus	27
B-1	Computer Program Flow Chart	45
B-2	Computer Program for IBM 1620 Computer	46
B-3	Computer Program for Time Sharing Computer	53
B-4	Computer Program for Time Sharing Computer	60

NOMENCLATURE

A	-	RADIUS OF THE CUT-BAR, FT
A_m	-	CROSS SECTIONAL AREA OF THE METER-BAR, FT^2
A_s	-	CROSS SECTIONAL AREA OF SPECIMEN BAR, FT^2
a	-	NON-DIMENSIONAL RADIUS, $\frac{A}{W}$
a_n	-	EULER COEFFICIENTS, $n = 1, 2, 3, \ldots$
B	-	OUTER RADIUS OF THE ANNULUS, FT
B_c	-	CRITICAL OUTER RADIUS OF THE ANNULUS, FT
b	-	NON-DIMENSIONAL OUTER RADIUS OF THE ANNULUS, $\frac{B}{W}$
b_n	-	EULER COEFFICIENTS, $n = 1, 2, 3, \ldots$
C_n	-	CONSTANTS, $n = 1, 2, 3, \ldots$
D_n	-	CONSTANTS, $n = 1, 2, 3, \ldots$
F_g	-	GEOMETRICAL FACTOR, DIMENSIONLESS
F_k	-	THERMAL CONDUCTIVITY FACTOR, DIMENSIONLESS
$G(Z)$	-	TEMPERATURES ALONG THE INNER CYLINDRICAL SURFACE OF THE ANNULUS, $^{\circ}F$
$g(u)$	-	NON-DIMENSIONAL TEMPERATURES ALONG THE INNER CYLINDRICAL SURFACE OF THE ANNULUS
$H(Z)$	-	TEMPERATURES ALONG THE OUTER CYLINDRICAL SURFACE OF THE ANNULUS, $^{\circ}F$
$h(u)$	-	NON-DIMENSIONAL TEMPERATURES ALONG THE OUTER CYLINDRICAL SURFACE OF THE ANNULUS
I_v	-	MODIFIED BESSEL FUNCTION OF THE FIRST KIND OF ORDER $v, v = 0, 1$
K_v	-	MODIFIED BESSEL FUNCTION OF THE SECOND KIND OF ORDER $v, v = 0, 1$
K_i	-	THERMAL CONDUCTIVITY OF THE POWER INSULATION OF THE ANNULUS, $\frac{BTU}{HR - FT\,^{\circ}F}$

K_m - THERMAL CONDUCTIVITY OF THE METER BAR, $\frac{BTU}{HR - FT\,^\circ F}$

K_s - THERMAL CONDUCTIVITY OF THE SPECIMEN BAR, $\frac{BTU}{HR - FT\,^\circ F}$

L - LENGTH OF THE SPECIMEN BAR, FT

l - NON-DIMENSIONAL LENGTH OF THE SPECIMEN BAR, $\frac{L}{W}$

M - LENGTH OF THE METER BAR, FT

m - POSITIVE INTEGER

n - POSITIVE INTEGER

P - RADIAL HEAT FLOW THROUGH THE INNER CYLINDRICAL SURFACE OF THE ANNULUS, $\frac{BTU}{HR}$

p - NON-DIMENSIONAL RADIAL HEAT FLOW

Q - AXIAL HEAT FLOW, $\frac{BTU}{HR}$

Q_i - AXIAL HEAT FLOW THROUGH THE AXIAL PLANE AT POSITION i IN THE CUT-BAR, $\frac{BTU}{HR}$

Q_T - TOTAL AXIAL HEAT FLOW WITH NO RADIAL LOSSES, $\frac{BTU}{HR}$

q - NON-DIMENSIONAL AXIAL HEAT FLOW

R - RESISTANCES, $\frac{HR - FT\,^\circ F}{BTU}$

r - RADIAL CYLINDRICAL COORDINATE VARIABLE, FT

S_m - TEMPERATURE GRADIENT IN THE METER-BAR, $\frac{^\circ F}{FT}$

S_s - TEMPERATURE GRADIENT IN THE SPECIMEN BAR, $\frac{^\circ F}{FT}$

S_i - TEMPERATURE GRADIENT AT POSITION i IN THE CUT-BAR, $\frac{^\circ F}{FT}$

T	-	TEMPERATURE AT THE SOURCE END OF THE APPARATUS, °F
u	-	NON-DIMENSIONAL AXIAL CYLINDRICAL COORDINATE VARIABLE
V	-	TEMPERATURE VARIABLE, °F
w	-	LENGTH OF THE CUT-BAR APPARATUS, FT
Z	-	AXIAL CYLINDER COORDINATE VARIABLE MEASURED FROM THE SOURCE END OF THE APPARATUS, FT
α	-	CONSTANT
γ	-	NET FRACTION OF POWER LOST OR GAINED IN THE CUT-BAR BETWEEN, $u = 0$ and $u = u_1$
θ	-	NON-DIMENSIONAL TEMPERATURE VARIABLE, $\frac{V - V_2}{V_1 - V_2}$
ρ	-	NON-DIMENSIONAL RADIAL CYLINDRICAL COORDINATE VARIABLE, $\frac{r}{w}$
σ_i	-	NON-DIMENSIONAL THERMAL CONDUCTIVITY OF THE POWER INSULATION OF THE ANNULUS, $\frac{K_i}{K_m}$
σ_s	-	NON-DIMENSIONAL THERMAL CONDUCTIVITY OF THE SPECIMEN BAR, $\frac{K_s}{K_m}$
ψ_m	-	NON-DIMENSIONAL TEMPERATURE GRADIENT IN THE METER-BAR, $\frac{S_m w}{T}$
ψ_s	-	NON-DIMENSIONAL TEMPERATURE GRADIENT IN THE SPECIMEN BAR, $\frac{S_s w}{T}$
Ω	-	NET FRACTION OF POWER LOST OR GAINED IN THE ANNULUS BETWEEN $u = 0$ and $u = u_1$

I. INTRODUCTION

The "Cut-Bar" technique of measuring thermal conductivity is a steady state comparative method which is most accurate in the low and intermediate temperature ranges for highly conductive materials. The schematic of the elements of a typical apparatus is illustrated in Figure 1. It consists of a pair of meter bars or discs between which a specimen is interposed. This composite bar is surrounded by an annulus of powder insulation which, in turn, is encased in a heated metal cylinder acting as a guard against extraneous heat losses. An axial heat flux is established by an isothermal source and sink at either end of the assembly.

For a first approximation, the determination of the specimen's conductivity is rather straightforward. Fourier's equation is written once for the average of the meter bar valves and once for the specimen:

$$Q/A\,\big|_m = K_m S_m \tag{1}$$

$$Q/A\,\big|_s = K_s S_s \tag{2}$$

where Q/A is the heat flux, k the thermal conductivity, and S the temperature gradient in the axial direction. By assuming the heat flow and cross-sectional areas constant throughout the composite bar the following relationship exists:

$$K_s = K_m \; [S_m/S_s] \tag{3}$$

where the temperature gradients are measured and the conductivity of the meter bar is known either by using a known standard material for the meter bar or by previous calibration with known standards as specimens.

Actually, the constant heat flow assumption is in error for two reasons; the radial heat exchange with the guard and the axial shunting exchange with the powder insulation caused by the difference in conductivities between the meter bars and specimen (Figure 2). A more realistic expression of the relative heat fluxes is:

$$KmS_m\,(1-\gamma_m) = K_s S_s\,(1-\gamma_s) \tag{4}$$

where γ is the ratio of the heat flow crossing the interface of the bar and insulation to the longitudinal heat flow in the bar if there were no losses (value in the bar a differential distance from the source). The evaluation of γ for a particular set of conditions may be done either analytically or experimentally. This report is concerned with an analytical solution.

FIGURE 1.

CUT-BAR APPARATUS WITH A LINEAR GUARD MATCHED AT THE ENDS

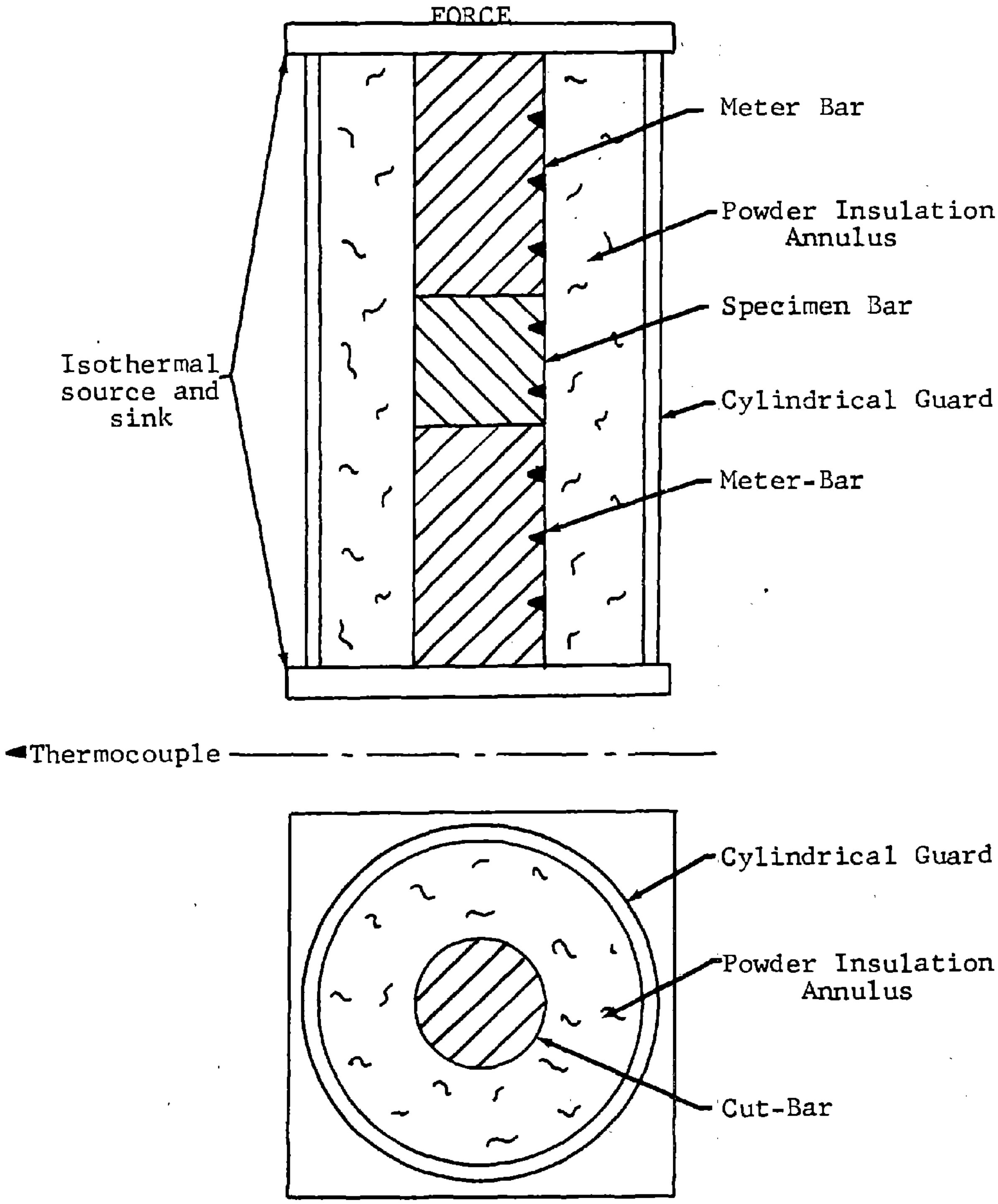

FIGURE 2

TEMPERATURES ON THE BOUNDARY SURFACES OF THE POWDER INSULATION ANNULUS

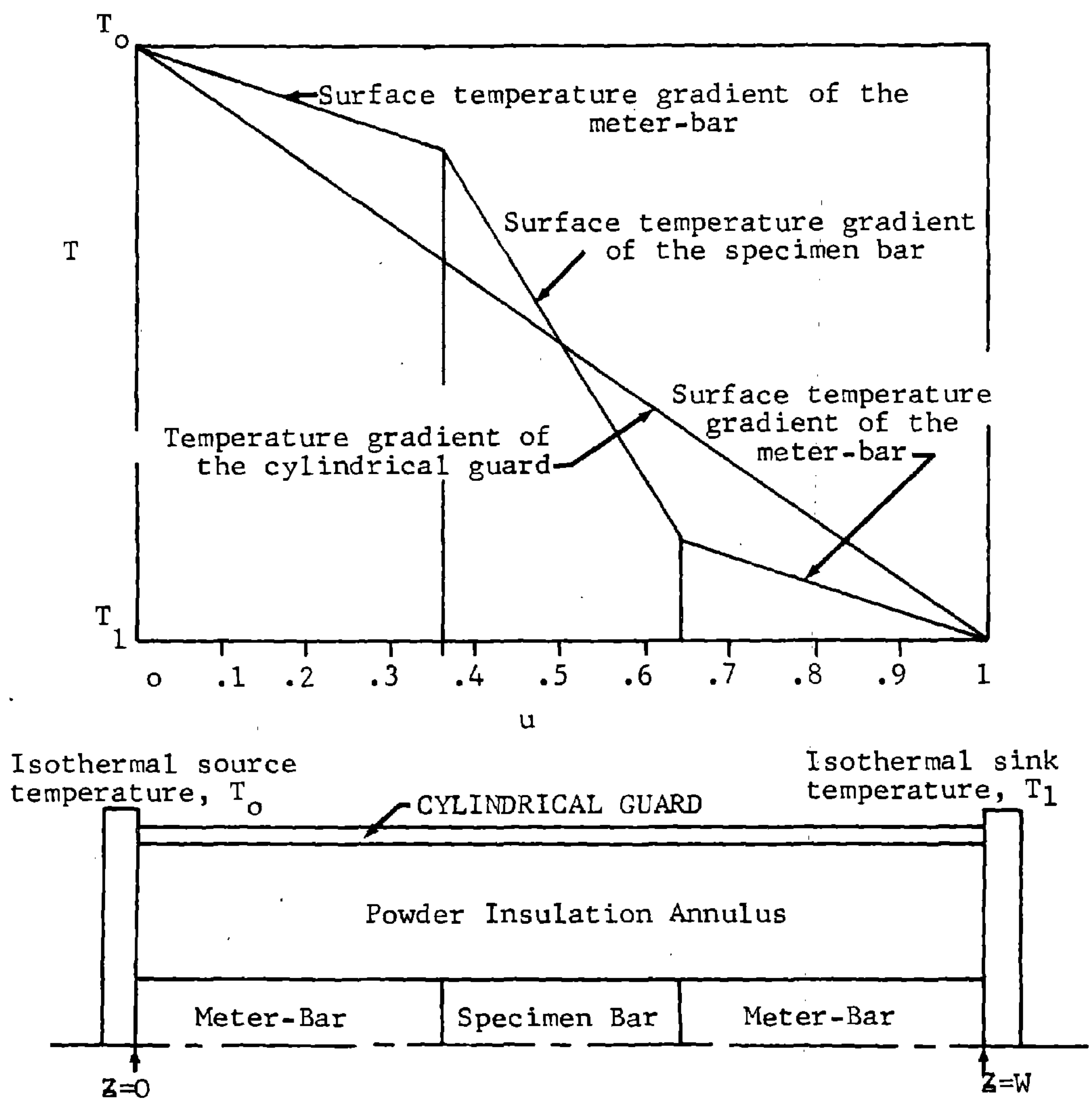

II. ANALYSIS

A theoritical evaluation of γ may be obtained by determining the heat flow across the interface of the bar and powder insulation. The heat conduction equation and boundary conditions for the annulus of insulation are assumed to be:

$$\frac{\partial^2\theta}{\partial \rho^2} + \frac{1}{\rho}\frac{\partial \theta}{\partial \rho} + \frac{\partial^2\theta}{\partial \mu^2} = 0 \tag{5}$$

$$\left.\begin{array}{llll} \rho = a & \theta = \dfrac{G(z) - \upsilon_2}{\upsilon_1 - \upsilon_2} \\ \rho = b & \theta = \dfrac{H(z) - \upsilon_2}{\upsilon_1 - \upsilon_2} \\ \mu = 0 & \theta = 1 \\ \mu = 1 & \theta = 0 \end{array}\right\} \tag{6}$$

Where the notation may be realized by reference to Figure 3 and the nomenclature section. The general solution to equation (5) is of course known (Reference [1]) and when applied to the particular boundary conditions the temperature distribution throughout the insulation is obtained. This distribution expression may be differentiated to obtain the radial gradient which in turn may be evaluated at the A radius boundary and then integrated along the A axis to get the total heat flow crossing the bar-insulation interface. Dividing this result by the longitudinal heat flow in the bar (assuming no losses) results in the following expression:

$$\gamma = k_i\left(\frac{1}{k_m} - \frac{1}{k_s}\right)\frac{2w}{\pi^2 A}\sum_{m=1}^{\infty}(-1)^m\left(\frac{1-\cos(2m\pi z)}{2m}\right)\mathrm{SIN}\left(\frac{m\pi L}{w}\right)$$

$$\left[\frac{K_o\left(\frac{2m\pi B}{w}\right) I_1\left(\frac{2m\pi A}{w}\right) + K_1\left(\frac{2m\pi A}{w}\right) I_o\left(\frac{2m\pi B}{w}\right)}{k_o\left(\frac{2m\pi B}{w}\right) I_o\left(\frac{2m\pi A}{w}\right) - K_o\left(\frac{2m\pi A}{w}\right) I_o\left(\frac{2m\pi B}{w}\right)}\right] \tag{7}$$

where the complete details of the above mentioned steps are presented in Appendix A. Equation (7) may be seperated into two terms of independent physical meaning, the conductivity and geometrical factors:

$$F_k = \left(k_i \frac{1}{k_m} - \frac{1}{k_s} \right) \tag{8}$$

$$F_g \equiv \frac{2w}{\pi^2 A} \sum_{m=1}^{\infty} (-1)^m \left(\frac{1-\cos(2m\pi Z)}{2m} \right) \mathrm{SIN} \left(\frac{m\pi}{w} L \right) \left[\frac{K_o\left(\frac{2m\pi B}{w}\right) I_1 \left(\frac{2m\pi A}{w}\right) + K_1 \left(\frac{2m\pi A}{w}\right) I_o \left(\frac{2m\pi B}{w}\right)}{K_o\left(\frac{2m\pi B}{w}\right) I_o \left(\frac{2m\pi A}{w}\right) \quad K_o \left(\frac{2m\pi A}{w}\right) I_o \left(\frac{2m\pi B}{w}\right)} \right] \tag{9}$$

Thus

$$\gamma = F_k \cdot F_g \tag{10}$$

Because of its complexity equation (9) has been programmed and is usually found to converge on a sufficiently accurate value in less than 150 terms. The flow chart and programs are presented in Appendix B. For a given apparatus F_g is seen to be a function of z only. However since the specimen length (L) effects the overall length (w) the actual values of $F_g(z)$ must be determined for each test. In Figure 4 a curve for particular inputs of w = 9.5 inches, A = 1 inch, B = 3 inches, L = 2 inches, represents the variation of the geometrical factor (F_g) with dimensionless distance (μ).

A reproduction of the computer program output can be seen in Figure 5 for one-half of the cut-bar. Since the ends of the cut-bar and guard are matched, the radial losses and gains are symmetrical about the center of the apparatus; the geometrical factor $F_g(Z)$ plotted over one-half of the cut-bar is a mirror image for the other half.

Finding F_k for the apparatus from equation (8) and using $F_g(Z)$ from the computer, the same curve with different ordinate scale will represent γ (Z).

In an earlier work (Reference 2), Flynn carried out an analysis for the case of the outer boundary temperature distribution equal to the inner boundary; that is, $H(Z) = G(Z)$. A comparison with this ideal case is made in Figure 6. The cut-bar apparatus with a matched guard has smaller geometrical factors compared with a similar apparatus and a linear guard matched at the ends, (Figure 6). The two cut-bar apparatus have the same dimensionless ratios, $\frac{L}{W} = 3$ and $\frac{L}{A} = 4$, and differ only in the thermal guarding. The relative flatness of the matched guard's correction curves, has the advantage of not having to average the correction factor between thermocouples discussed in the example in Chapter III. Furthermore, as the ratio $\frac{B}{A}$ decreases in the linear guard apparatus, the geometrical factor will increase to a very large number. Conversely, letting $\frac{B}{A}$ decrease in the matched guard apparatus, the geometrical factor will decrease, and in the limit as $\frac{B}{A}$ approaches one, F_g approaches zero. There phenomena are better illustrated in Figure 7, which is a plot of the maximum geometrical factors (at the mid-horizontal plane) against the ratio of the guard and bar radii. The linear guard's increasing geometrical factor with decrease of $\frac{B}{A}$ may be explained with the decreasing insulating resistance, the radial losses begin to approach the axial flux. The matched guard apparatus has a minimum of radial losses; thus, letting $\frac{B}{A} \rightarrow 1$ decreases the shunting loss by decreasing the medium through which it takes place. The conditions of the zero limit are, of course, quite impractical.

It may be concluded that although the errors associated with the linear guard are of greater magnitude and variation along the longitudinal axis, than that for a matched guard, they are not excessive for large $\frac{B}{A}$ ratios. Consequently, this method may still be the preferred technique; particularly, when considering the additional complexity and cost of the matched guard's experimental apparatus. The details of how to design and correct a linear guard apparatus are discussed in Chapter III.

FIGURE 3

SHUNTING OF HEAT FLUX IN A
CUT-BAR APPARATUS

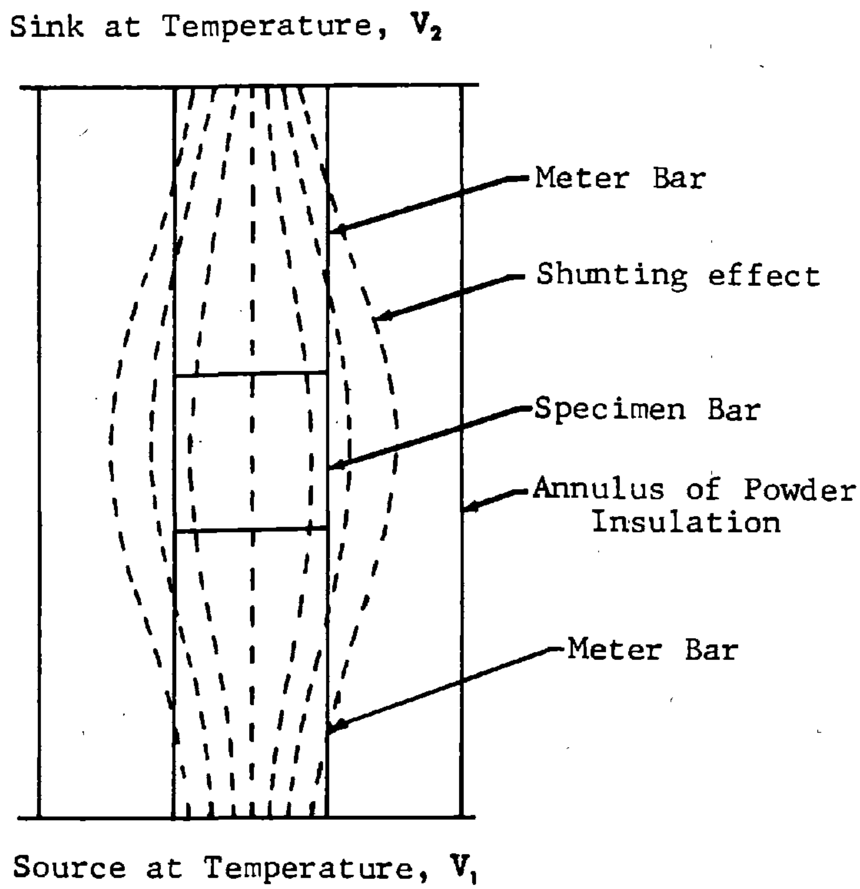

FIGURE 4

PLOT OF THE GEOMETRICAL FACTOR ON THE LEFT SCALE AND FRACTIONAL POWER CHANGE ON THE RIGHT SCALE OF THE ORDINATE AXIS VERSUS THE DIMENSIONLESS LENGTH u ON THE AXIS OF THE ABSCISSA

Dimensionless parameters for this apparatus are:
$\frac{L}{A} = 2.$, $\frac{L}{W} = .2105$, $\frac{B}{A} = 3.$, $\frac{K_i}{K_s}=.01111$, $\frac{K_i}{K_m}=.001111$

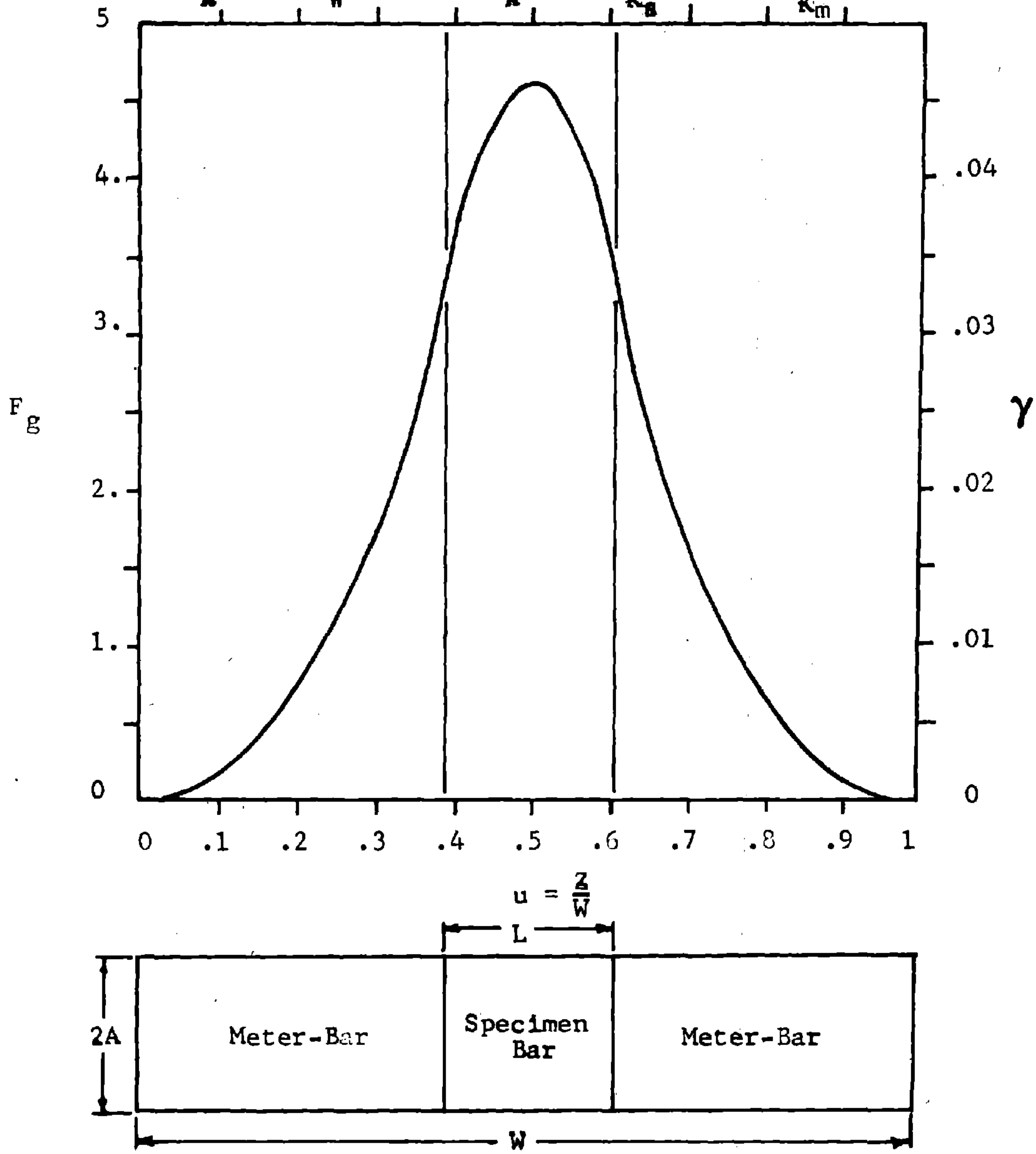

FIGURE 5

COMPUTER OUTPUT

RESULTS OF POWER LOSS OVER LENGTH OF METER-BAR

F_g VERSUS Z FOR 20 POINTS FROM Z=0 TO END

W	A	B	L	TEST	P	M	F
9.50000	1.00000	3.00000	2.00000	.00010	20	150	19

POINT	Z	KL	SER	F_g	M=150
1	.23750	3	.0057214	.0110143	
2	.47500	59	.0228464	.0439817	
3	.71250	3	.0514361	.0990198	
4	.95000	3	.0915257	.1761964	
5	1.18750	21	.1433035	.2758740	
6	1.42500	3	.2069009	.3983055	
7	1.66250	21	.2825233	.5438862	
8	1.90000	3	.3706142	.7134703	
9	2.13750	21	.4717329	.9081341	
10	2.23750	21	.5867708	1.1295939	
11	2.61250	21	.7170570	1.3804081	
12	2.85000	3	.8646966	1.6646296	
13	3.08750	1	1.0334212	1.9894417	
14	3.32500	2	1.2303858	2.3686188	
15	3.56250	0	1.4725646	2.8348377	
16	3.80000	0	1.8485560	3.5586596	
17	4.03750	0	2.1179562	4.0772827	
18	4.27500	2	2.2792856	4.3878582	
19	4.51250	0	2.3698414	4.5621874	
20	4.75000	2	2.3992300	4.6187635	

FIGURE 6

COMPARISON OF THE GEOMETRICAL FACTORS FOR A CUT-BAR APPARATUS HAVING A MATCHED GUARD WITH AN APPARATUS HAVING A LINEAR GUARD MATCHED AT THE ENDS

The dimensionless variables of the apparatus are: $\frac{L}{W} = 3$, $\frac{L}{A} = 4$

L. G. - Linear guard matched at the ends
M. G. - Matched Guard

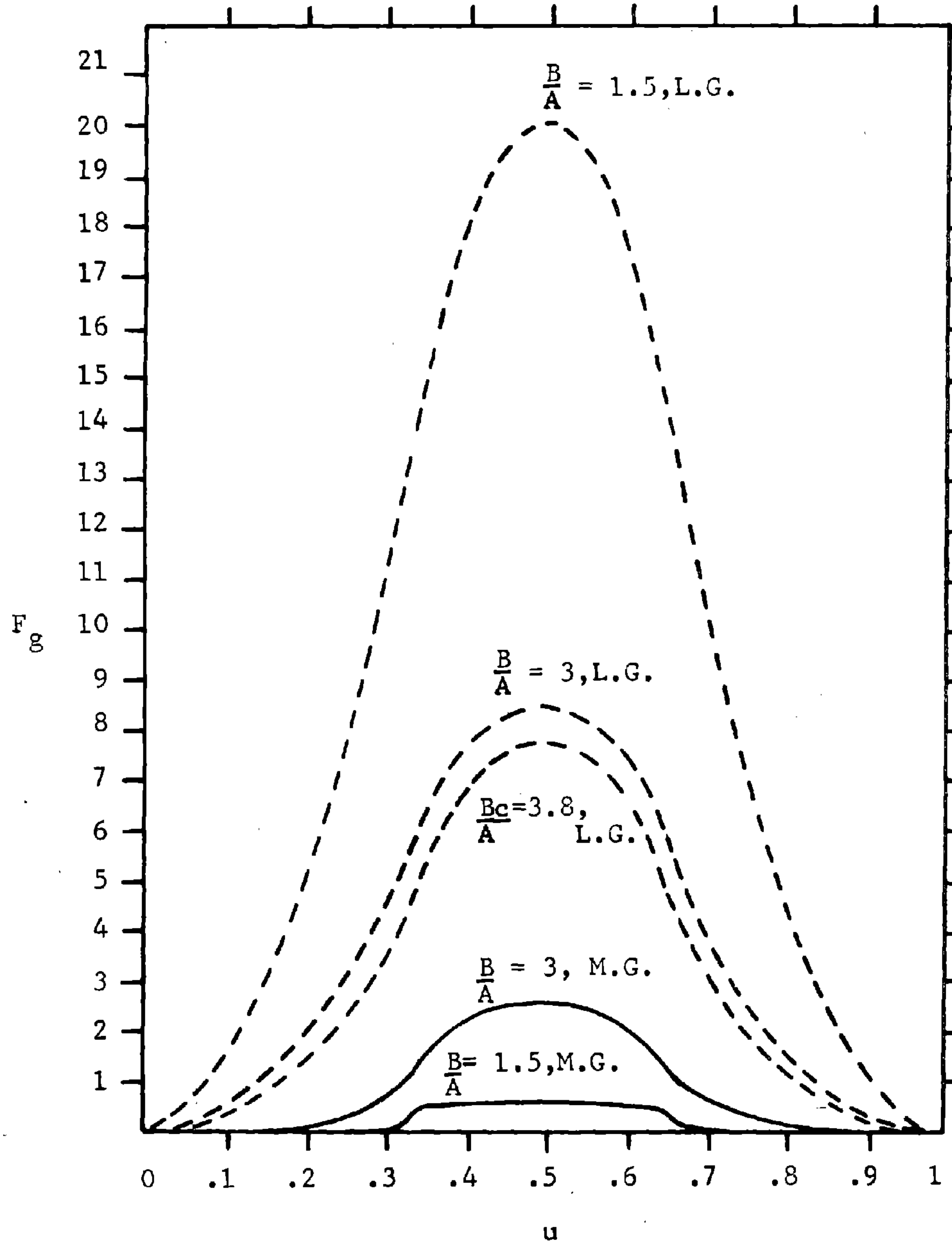

FIGURE 7

GEOMETRICAL FACTOR AS A FUNCTION OF THE RATIO OF APPARATUS DIAMETERS

Plot of the geometrical factor as a function of the ratio of guard and specimen diameters for a matched guard and a linear guard matched at ends.

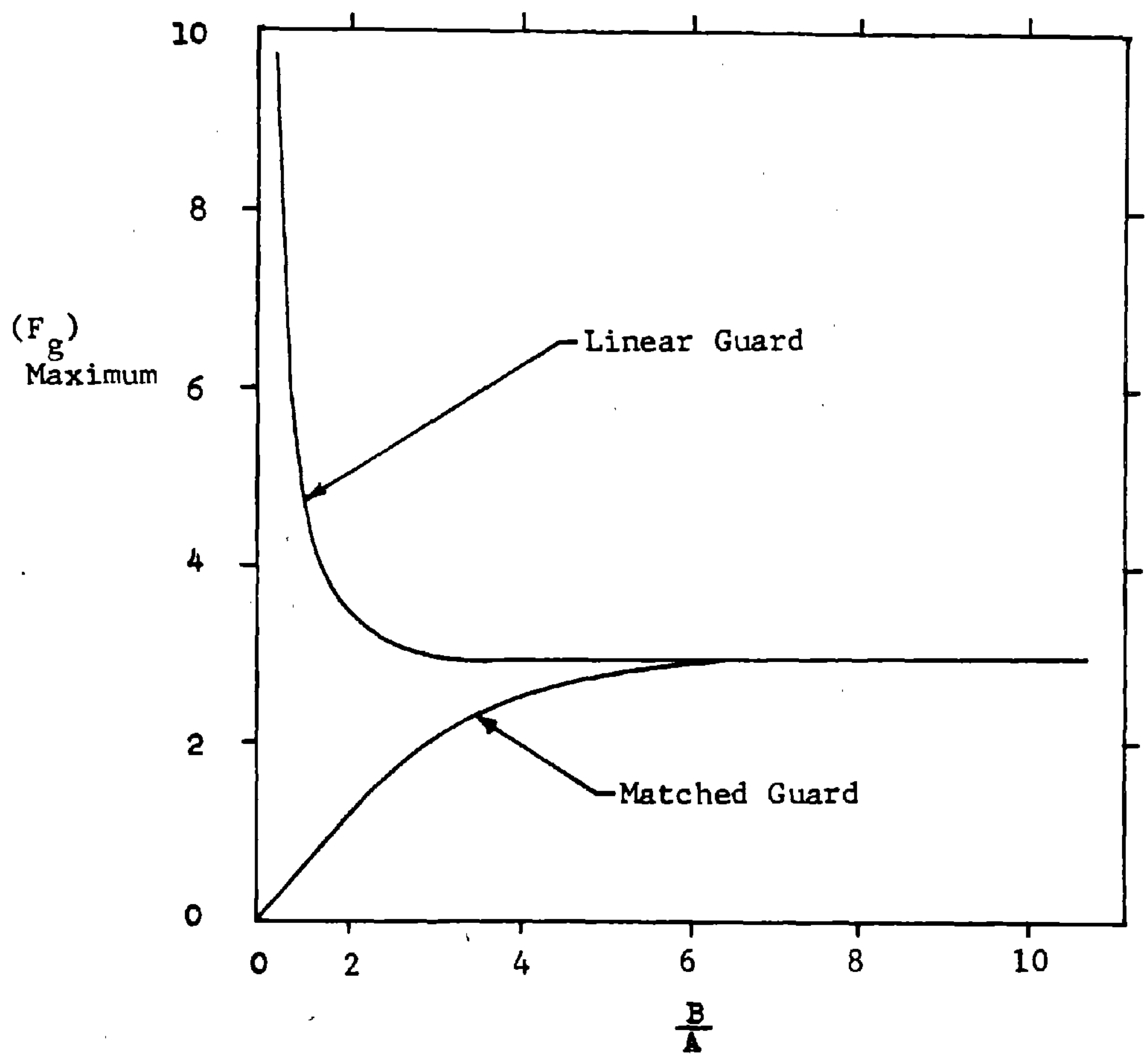

III. DESIGN

The computer results of equation (9) are also plotted as design charts. The design charts can be used to find optimum dimensions for a test setup. A larger than practical range of variables are shown, so that the designer can be sure of an optimum. It should be noted that in the development of the design charts, the only dimensionless parameters are those with physical implications.

The design chart (Figure 8) plots the geometrical factor F_g against the radii ratio of guard to bar $\frac{B}{A}$, using specimen length to specimen radius $\frac{L}{A}$, and overall length $\frac{L}{W}$, as parameters. The geometrical factor F_g, should be kept to a minimum to obtain the optimum design. It is evident from equation (9) that as $\frac{B}{A}$ approaches 1, F_g approaches infinity as a limit for any $\frac{L}{A}$ and $\frac{L}{W}$. However, as $\frac{B}{A}$ increases F_g rapidly settles down to various asymptotic values. An arbitrary curve designated B_c is drawn from a locus of points in the family of curves for $\frac{L}{A}$ and $\frac{L}{W}$ where the slope of these curves have an absolute value of 0.01. An increase in the ratio $\frac{B}{A}$, passed the ratio $\frac{B_c}{A}$ does not significantly decrease F_g. Thus, $\frac{B_c}{A}$ may be considered as points of diminishing return and are the recommended value for optimum design.

Figure 9 is a plot of F_g against $\frac{L}{W}$ for an $\frac{L}{A}$ family of curves. It also has a scale on the right ordinate of $\frac{B_c}{A}$. If the designer uses $\frac{B_c}{A}$ as the sizing of the annulus, he may immediately find the minimum geometrical factor F_g, for whatever values of $\frac{L}{W}$ and $\frac{L}{A}$ he desires. It may be seen in Figure 9, that as $\frac{L}{W}$ approaches the limit $\frac{L}{W} = 1$, $F_g \rightarrow 0$ for all values of $\frac{L}{A}$. When $\frac{L}{W} = 1$, the cut-bar is a solid bar composed of the specimen material; similarly, when $L = 0$, the cut-bar is a solid bar, but composed of meter bar material. In both cases, there is an axial temperature gradient in the cut-bar which matches the axial temperature gradient in the guard. Therefore, F_g must be zero, because there is neither a radial heat flow nor a shunting flow in the annulus.

The effect of varying the specimen thermal conductivity on the thermal conductivity factor, F_k, (Figure 10) can be seen by using equation (8) to plot F_k against $\frac{K_s}{K_i}$ for various ratios of $\frac{K_m}{K_i}$. The plotted quantities go through zero at $\frac{K_s}{K_i} = \frac{K_m}{K_i}$, then approach ∞ as $\frac{K_s}{K_i}$ becomes small, and asymptotically approach $-\frac{K_i}{K_m}$ as $\frac{K_s}{K_i}$ becomes large.

Since a designer would choose a geometrical factor which would be small, he could multiply the ordinary scale of Figure 10 to obtain γ. The ordinate would be the measure of thermal conductivity of materials in terms of fractional power gained or lost in the cut-bar apparatus.

If it is necessary to measure a large range of specimen thermal conductivities with a single pair of meter-bars, the conductivity of the meter-bar should be in the lower end of the range. To have a minimal thermal conductivity factor range, for a given range of specimen materials using only a single pair of meter-bars, it is necessary to find the arithmetic average of the resistance of the specimen range. The arithmetic average of the maximum and minimum of the specimen resistance range will be used as the optimum resistance for the meter-bar.

Therefore,

$$R_m = 1/2 \left[\left(R_s\right)_{max} + \left(R_s\right)_{min} \right] \tag{11}$$

Substituting the equivalent thermal conductivity for resistance, that is, $R = \frac{1}{K}$, into equation (11)

it becomes,

$$K_m = \frac{2\left(K_s\right)_{max} \left(K_s\right)_{min}}{\left(K_s\right)_{max} + \left(K_s\right)_{min}} \tag{12}$$

$(K_s)_{max}$ and $(K_s)_{min}$ are the maximum and minimum specimen thermal conductivities to be measured.

The maximum fractional power is approximately,

$$\gamma_{max} = \pm \frac{K_i}{2} \left[\frac{1}{(K_s)_{min}} - \frac{1}{(K_s)_{max}} \right] F_g \tag{13}$$

When $(K_s)_{max}$ is very large relative to $(K_s)_{min}$, equation (12) is approximately,

$$K_m \doteq 2\ (K_s)_{min} \tag{14}$$

For the maximum fractional power change over the range, equation (13) becomes,

$$\gamma_{max} = \pm \frac{K_i}{2\ (K_s)_{min}} F_g \tag{15}$$

Figure 11 shows the table with several ranges of thermal conductivity; the preferred meter-bar for each range, and the maximum fractional power change associated for a given geometrical factor of 1.0, and an insulation thermal conductivity of

$$.058 \ \frac{\text{BTU}}{\text{HR-FT}^{\text{o}}\text{F}}.$$

To illustrate the fractional power change that would arise if a range of materials for the specimen bar were measured using the same meter-bar and insulation annulus, γ is plotted against dimensionless length in Figure 12. The geometrical dimensions of the cut-bar apparatus in Figure 12 are the dimensions used for the F_g values to obtain a plot of γ versus the dimensionless length u. The quantity γ (u) is shown for specimens having a thermal conductivity ranging from one-tenth to ten times that of the meters.

The following is an example problem, illustrating the use of the design charts and equations of a cut-bar apparatus having an optimal design using a minimal fractional power change. The fractional power change is dependent on both the geometrical factor and the thermal conductivity factor, while the geometrical and thermal conductivity factors are independent of one another. Thus, these factors are each minimized separately.

Assuming that the particular design requirements are limited to an overall length of w equal to 9.5 inches, with the specimen dimensions of length L equal to 2 inches, and specimen radius A equal to 1 inch, the specimen thermal conductivity will have a range from a minimum of 4.5 $\frac{\text{BTU}}{\text{HR-FT}^{\text{o}}\text{F}}$ to a maximun of 242 $\frac{\text{BTU}}{\text{HR-FT}^{\text{o}}\text{F}}$ (the range of most metals).

From the above known dimensions: $\frac{L}{A} = 2$ and $\frac{L}{W} = .2111$. The design chart in Figure 9 indicates the dimensionless ratio $\frac{B_c}{A}$ is found to be $\frac{B_c}{A} = 4.06$ or $B_c = 4.06$ inches. Thus, the guard diameter should be at least 4 inches or greater.

The computer program in Appendix B is used to calculate the geometrical factor for 20 points along the cut-bar. The computer program stops when the geometrical factor has converged within the test range of .0001 or reaches the maximum number of series terms of M equal to 150. The frequency F of the test for convergency occurs every 7 terms in the series.

The inputs into the computer program are: W = 9.5 inches; A = 1.0 inch; B = 4.06 inches; L = 2.0 inches; Test = .0001; P = 20 points; M = 150 terms, and F = 7. The resulting output from the computer program is illustrated in Figure 13. Calculated for each point is the distance Z of that point in inches from the reference end, the number of KL terms before the last term in the series is calculated, the value of the SER series summation, and the value for the geometrical factor F_g. The resulting output for 20 points along one symmetrical half of the cut-bar is presented in Figure 13. From this output of the computer program, a graph (Figure 14) is drawn for F_g versus Z. In Figure 14, F_g is on the left scale of the ordinate axis and its maximum value at the center of the cut-bar is 4.31.

Since the apparatus is to be used to measure the thermal conductivity of specimens ranging from Bismuth to that of Silver, the limiting conductivity values are $(K_s)_{min} = 4.5 \frac{BTU}{HR\text{-}FT^oF}$ and $(K_s)_{max} = 242 \frac{BTU}{HR\text{-}FT^oF}$. The insulation best suited for the apparatus has a value of $K_i = .1 \frac{BTU}{HR\text{-}FT^oF}$. Using equation (12), K_m is calculated as 9 $\frac{BTU}{HR\text{-}FT^oF}$, which is in the range of stainless steels. Using the above values for K_i, $(K_s)_{min}$, $(K_s)_{max}$ and $(F_g)_{max}$ and substituting these values into equation (13), the maximum value of the fractional power change is -.047 which is at the center of the specimen bar.

To calculate the fractional power change for a specific test the apparent conductivity is first used, for instance $K_s = 90 \frac{BTU}{HR\text{-}FT^oF}$. Knowing K_i and K_m the conductivity factor F_k is found to be .01 from equation (8). Since the geometrical factor has been plotted for the apparatus in Figure 14, the fractional power change can be found by changing the scale on the axis of the ordinate by a factor of .01, and this scale is shown on the right scale on the axis of the ordinate.

Since the temperature gradients are calculated between two thermocouples placed a finite distance apart, the fractional power changes γ_m and γ_s which are used in equation (4) represent the average fractional power changes between the measuring stations, this average γ can be calculated as,

$$\gamma \text{ aver} = \frac{\int_{Z_1}^{Z_2} \gamma \, dZ}{Z_2 - Z_1}$$

To find the average γ to be used for γ_m in this example, (referring to Figure 14) the cross-hatched area under the curve from $Z_1 = 1.1875$ to $Z_2 = 3.325$ inches, is measured by counting graph squares with the result that $\gamma_m = .01025$.

γ_s is calculated by using the same graphical procedure with the two measuring thermocouples being at points $Z_1 = 4.037$ and $Z_2 = 5.463$ on the specimen bar; thus γ_s is .0414.

The fractional power change for γ_m and γ_s is then substituted into equation (4), where $K_m = 9 \frac{BTU}{HR\text{-}FT^oF}$. The resulting equation, to find the thermal conductivity of the specimen for the example problem, is,

$$K_s = 8.72 \frac{S_m}{S_s}$$

S_m and S_s are determined from the measurements of the thermocouples.

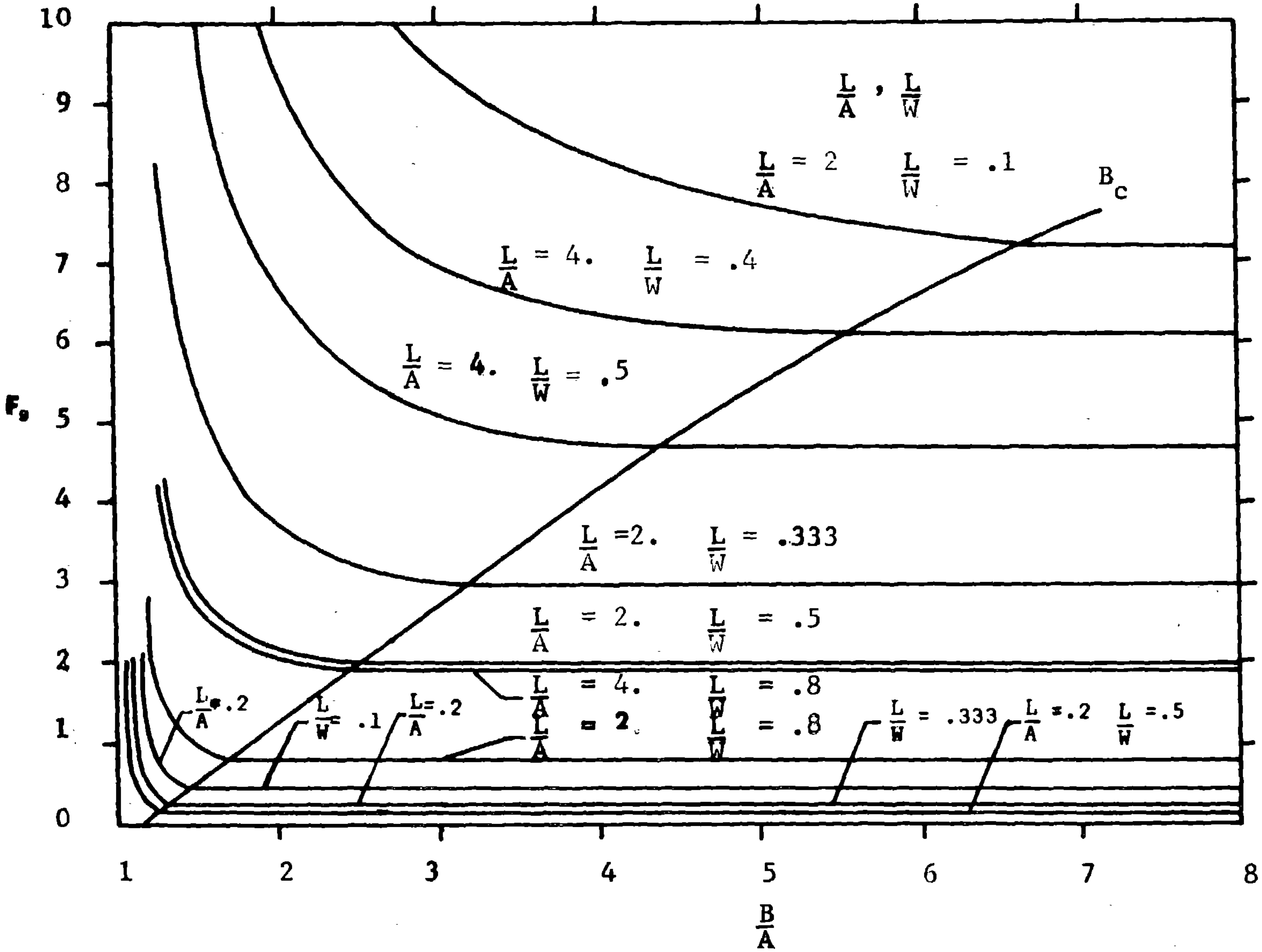

FIGURE 8

DESIGN CHART

FIGURE 9

DESIGN CHART FOR THE OPTIMUM DIMENSIONLESS

RATIO $\frac{B}{A}$, VARYING THE DIMENSIONLESS

VARIABLES $\frac{L}{A}$ AND $\frac{L}{W}$

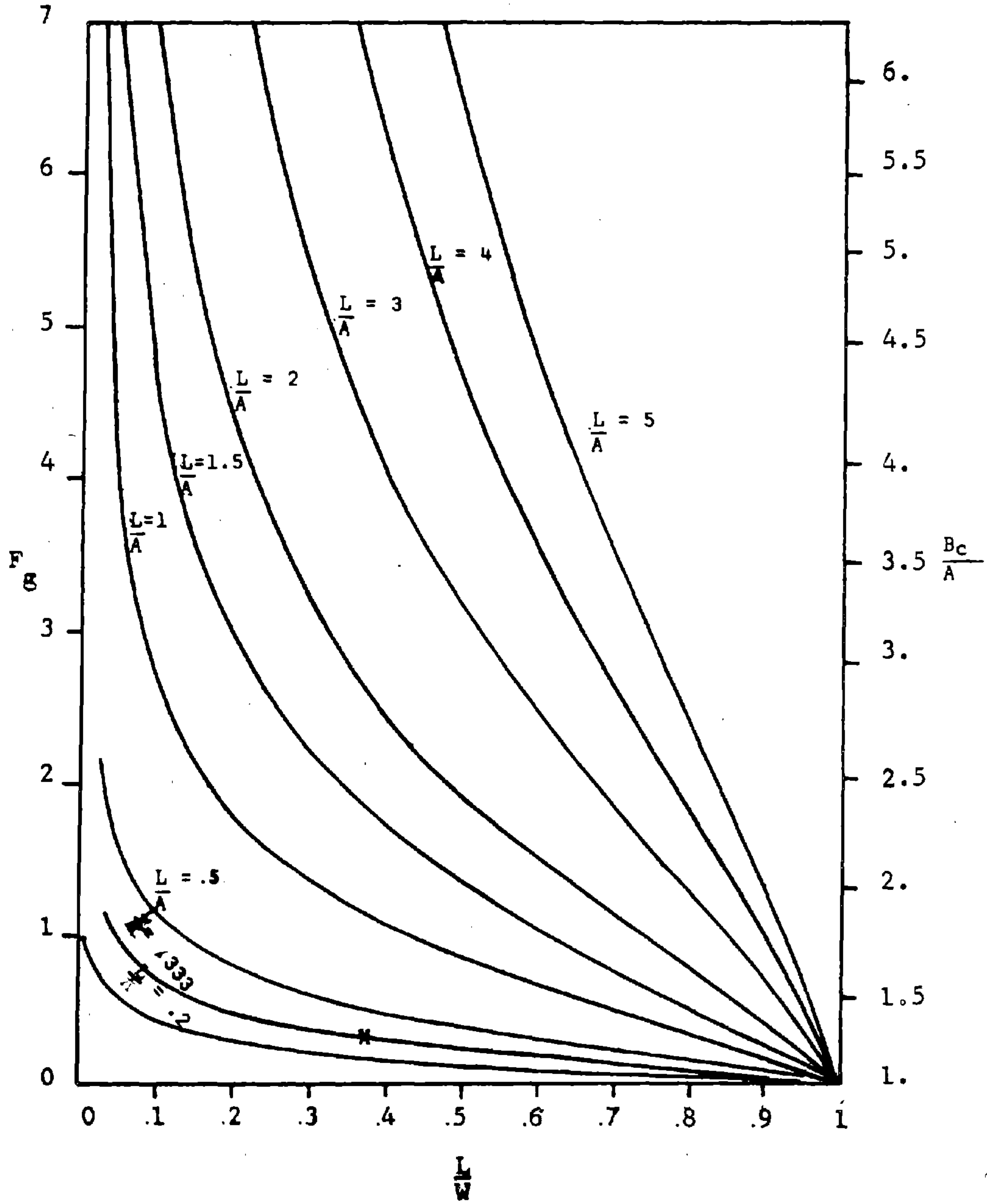

FIGURE 10

EFFECT OF SPECIMEN THERMAL CONDUCTIVITY ON THE THERMAL CONDUCTIVITY FACTOR FOR A RANGE OF DIMENSIONLESS RATIOS

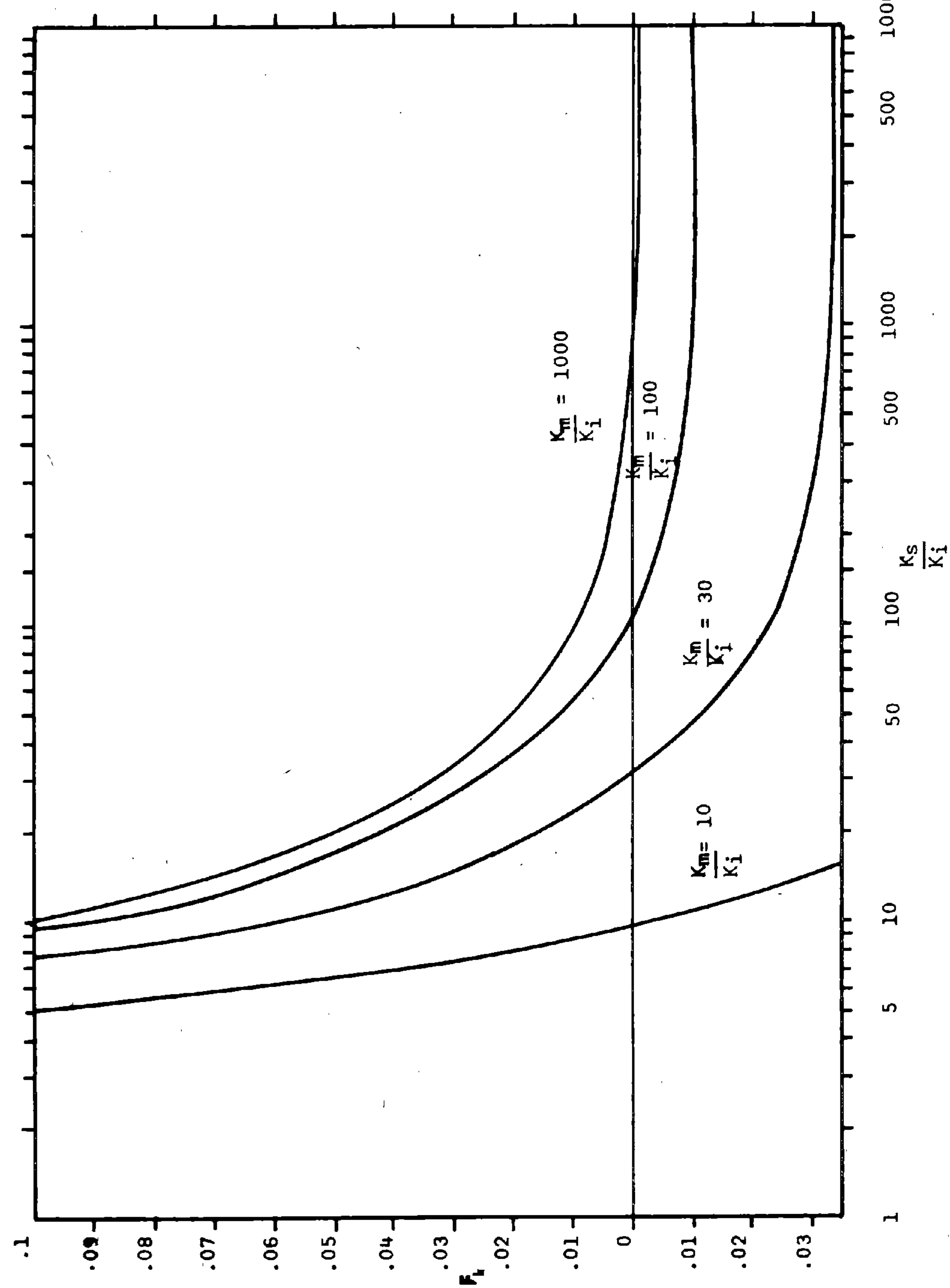

FIGURE 11

MAXIMUM ERRORS FOR VARIOUS RANGES OF

SPECIMEN THERMAL CONDUCTIVITY

Minimum	Maximum	Optimal K_m	Maximum Error in K_s Range
$\frac{BTU}{HR\text{-}FT^{o}F}$	$\frac{BTU}{HR\text{-}FT^{o}F}$	$\frac{BTU}{HR\text{-}FT^{o}F}$	$\pm$ %
0.2889	0.5779	0.3872	5.0
.5779	.8669	.6935	1.7
.5779	1.1558	.7686	2.5
.5779	2.8896	.9651	4.0
.5779	5.7793	1.0518	4.5
.5779	57.7934	1.1443	5.0
2.8896	5.7793	3.8548	.50
2.8896	28.8967	5.2534	.90
5.7793	28.8967	9.0753	.40
5.7793	57.7934	10.5183	.45
5.7793	577.9340	11.4430	.50
57.7934	577.9340	105.1839	.045

FIGURE 12

PLOT OF FRACTIONAL POWER CHANGE FOR A RANGE OF SPECIMEN THERMAL CONDUCTIVITIES VERSUS DIMENSIONLESS LENGTH

Dimensionless parameters for this apparatus are: $\frac{L}{A} = 2$; $\frac{L}{W} = .2105$; $\frac{B}{A} = 3$

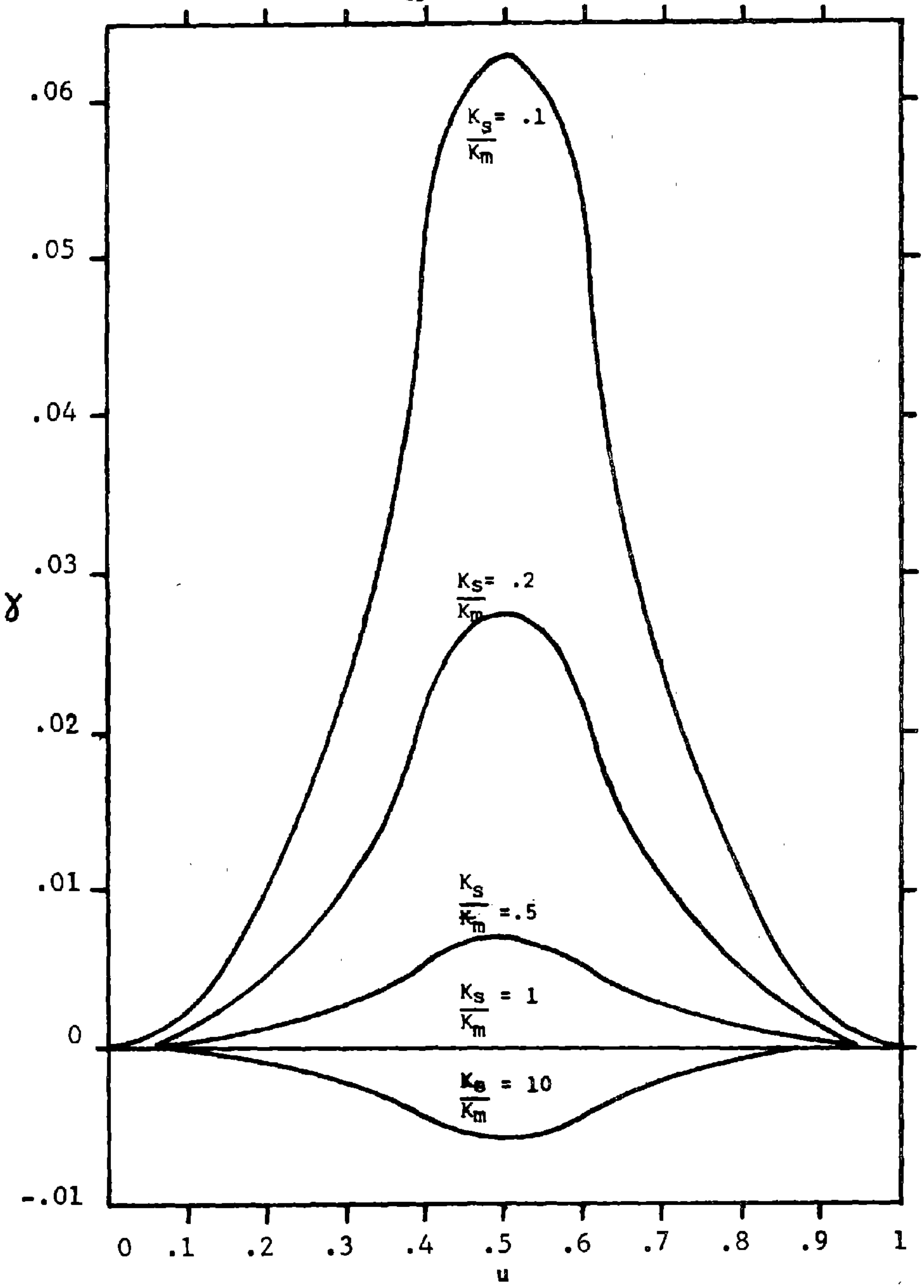

FIGURE 13

COMPUTER OUTPUT

RESULTS OF POWER LOSS OVER LENGTH OF METER-BAR

F_g VERSUS Z FOR 20 POINTS FROM Z=0 TO END

W	A	B	L	TEST	P	M	F
9.50000	1.00000	4.06000	2.00000	.00010	20	150	7

POINT	Z	KL	SER	F_g	M=150
1	.23750	56	.0047517	.0091476	
2	.47500	35	.0193526	.0372558	
3	.71250	49	.0436508	.0840324	
4	.95000	35	.0778525	.1498741	
5	1.18750	35	.1221891	.2352265	
6	1.42500	35	.1769584	.3406630	
7	1.66250	21	.2425952	.4670207	
8	1.90000	42	.3197168	.6154876	
9	2.13750	42	.4089831	.7873344	
10	2.37500	21	.5115743	.9848330	
11	2.61250	49	.6291793	1.2112346	
12	2.85000	21	.7643035	1.4713626	
13	3.08750	7	.9209332	1.7728908	
14	3.32500	2	1.1064501	2.1300297	
15	3.56250	1	1.3382798	2.5763256	
16	3.80000	0	1.7053046	3.2828861	
17	4.03750	0	1.9674043	3.7874549	
18	4.27500	2	2.1233365	4.0876404	
19	4.51250	3	2.2105791	4.2555913	
20	4.75000	7	2.2389335	4.3101764	

FIGURE 14

PLOT OF THE GEOMETRICAL FACTOR ON THE LEFT SCALE AND FRACTIONAL POWER CHANGE ON THE RIGHT SCALE OF THE ORDINATE AXIS VERSUS THE Z ON THE AXIS OF THE ABSCISSA

Dimensions of this apparatus are:

W = 9.5 in., A = 1 in., B = 4.06 in., L = 2. in.,

$K_i = .01 \frac{BTU}{HR\text{-}FT^oF}$, $K_s = 90 \frac{BTU}{HR\text{-}FT^oF}$, $K_m = 9 \frac{BTU}{HR\text{-}FT^oF}$

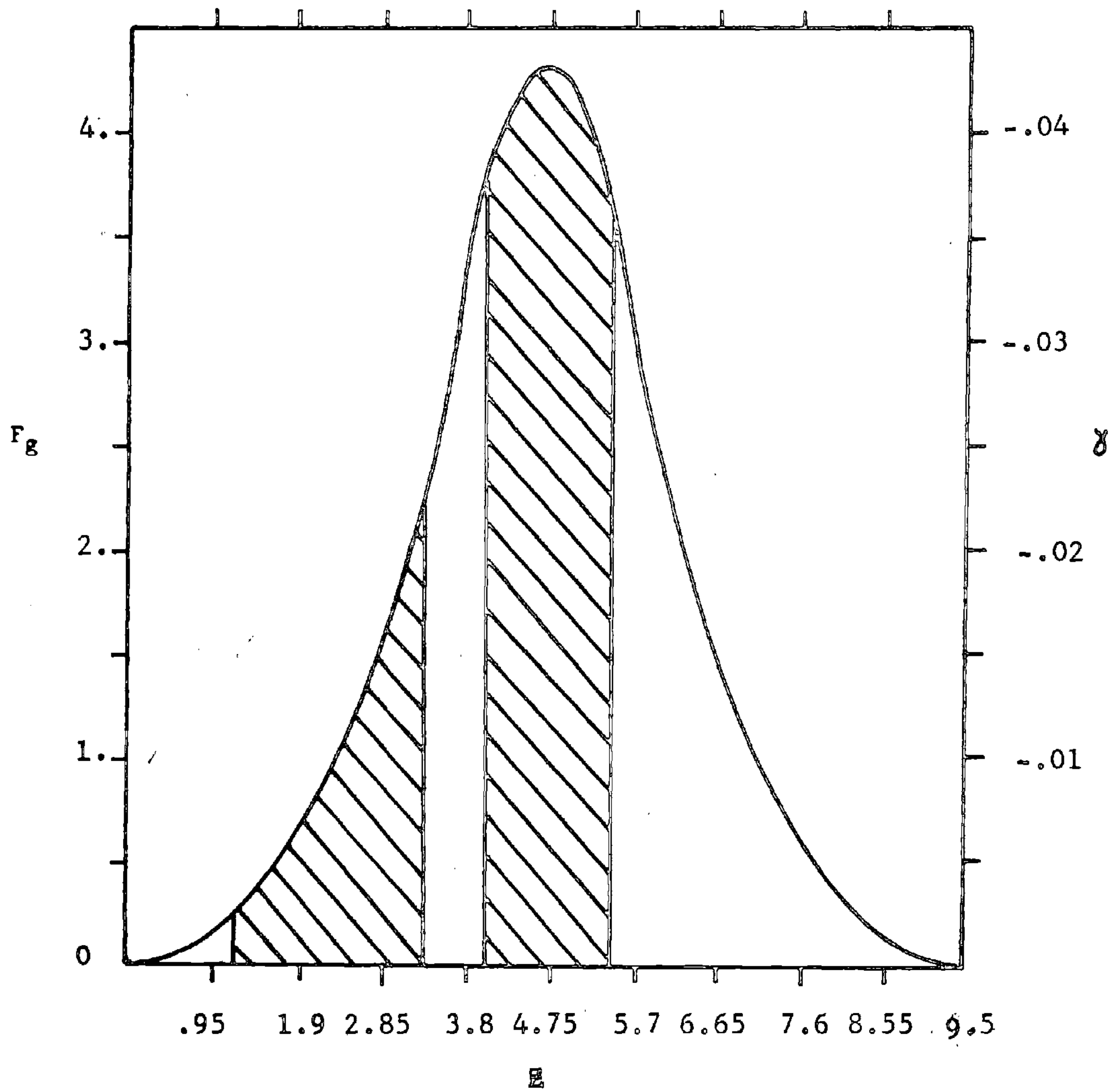

IV. REFERENCES

[1] Carslaw and Jaeger. Conduction of Heat in Solids. Second Edition. London: Oxford University Press, 1959, pp. 214-229.

[2] Flynn, D. R. "Thermal Guarding of Cut-Bar Apparatus." Technical notes of the Conference on Thermal Conductivity Methods. Battelle Memorial Institute, Columbus, Ohio. October 26, 27, 28, 1961., pp. 133-150

[3] Robinson, H.E. "Thermal Conductivity Reference Standards." Proceedings of the Second Conference on Thermal Conductivity. Division of Applied Physics, National Research Council, Ottaws, Canada. October 10, 11, 12, 1962, pp. 311-322.

APPENDIX A

MATHEMATICAL ANALYSIS OF GEOMETRICAL FACTOR

It is important to note that this analysis is based on the change of heat flow in the annulus and through the boundaries of the annulus, so the equations and solution are based only on the annulus, and not on the cut-bar or the cylindrical guard; however, the boundary conditions are based on the temperature distribution of the cut-bar, the cylindrical guard, and the heater cooler system.

Mathematical investigation of the powder insulation annulus follows:

Figure A-1 shows a schematic of the cut-bar apparatus. The two meter bars are of equal length M and of the same thermal conductivity K_m.

W - the overall length of the cut-bar

M - the length of the meter-bar

L - the length of the specimen bar

A - the radius of the cut-bar, or the inner radius of the powder insulation annulus

B - the outer radius of the powder insulation annulus or the inner radius of the cylindrical guard.

K_m - the thermal conductivity of the meter-bar

FIGURE A-1

A SCHEMATIC OF THE CUT-BAR APPARATUS

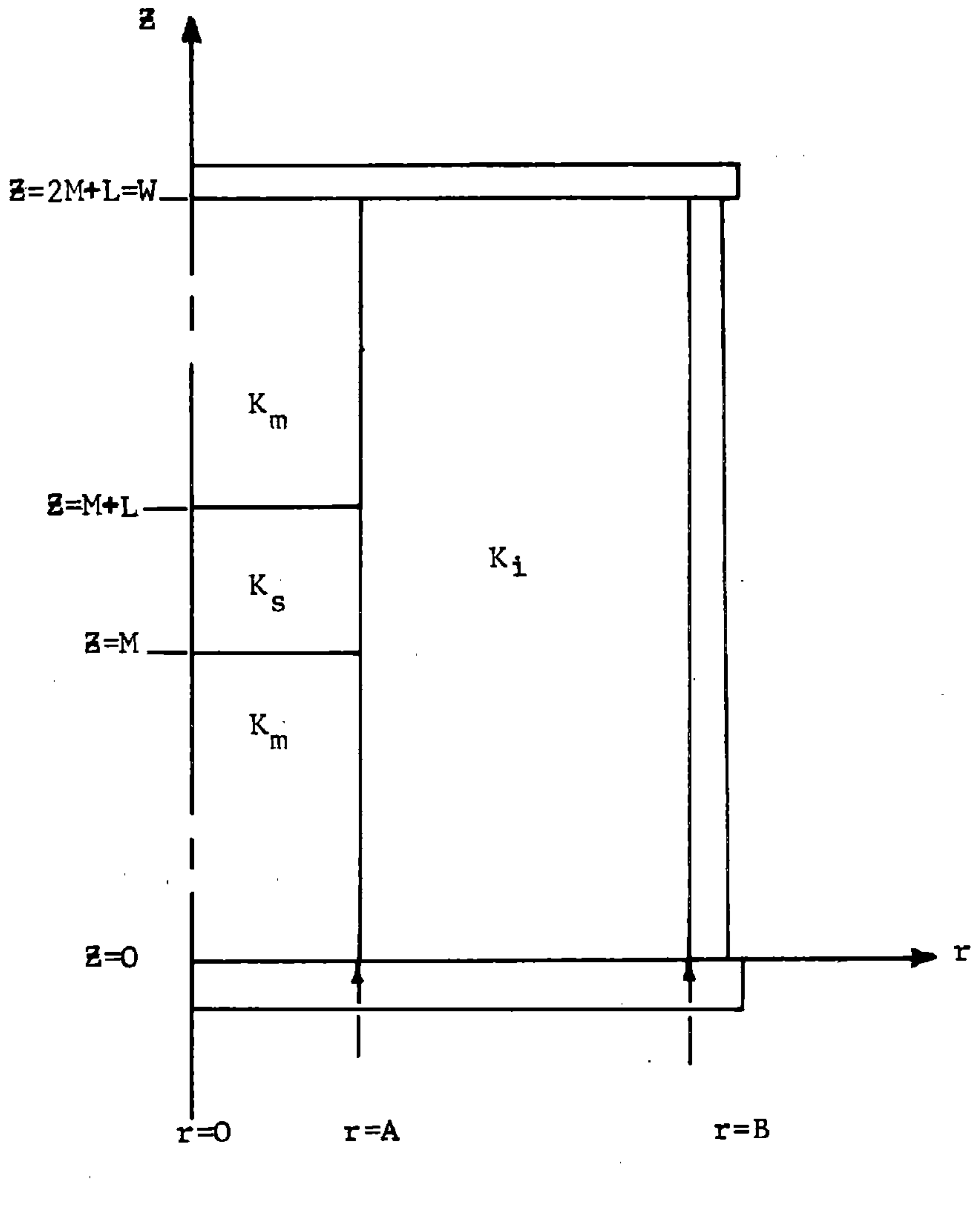

K_s - the thermal conductivity of the specimen bar

K_i - the thermal conductivity of the powder insulation in the annulus

V - the temperature variable

The boundary conditions of the powder insulation annulus are:

$$
\begin{array}{lll}
r = A & 0 \leq Z \leq W & V = G(Z) \\
r = B & 0 \leq Z \leq W & V = H(Z) \\
A = r = B & Z = 0 & V_1 = V = \text{Constant} \\
 & & G(0) = H(0) = V_1 \\
A \leq r \leq B & Z = W & V = V_2 = \text{Constant} \\
 & & G(W) = H(W) = V_2
\end{array}
\qquad (A\text{-}1)
$$

The above boundary conditions of the annulus may be reduced to dimensionless variables.

The dimensionless variables are:

$$
\begin{array}{lll}
u = \dfrac{Z}{W} & m = \dfrac{M}{W} & \ell = \dfrac{L}{W} \\[2ex]
\rho = \dfrac{r}{w} & a = \dfrac{A}{W} & b = \dfrac{B}{W} \\[2ex]
\theta = \dfrac{V - V_2}{V_1 - V_2} & \sigma_s = \dfrac{K_s}{K_m} & \sigma_i = \dfrac{K_i}{K_m}
\end{array}
\qquad (A\text{-}2)
$$

The dimensionless boundary conditions are:

$$\rho = a \qquad 0 \leq u \leq 1 \qquad \theta = g(u) = \frac{G(Z)-V_2}{V_1 - V_2}$$

$$\rho = b \qquad 0 \leq u \leq 1 \qquad \theta = h(u) = \frac{H(Z)-V_2}{V_1 - V_2}$$

$$a = \rho = b \qquad u = 0 \qquad \theta = 1$$

$$a = \rho = b \qquad u = 1 \qquad \theta = 0 \tag{A-3}$$

The governing differential equation of heat flow in the annulus is Laplace's equation in cylindrical coordinates:

$$\nabla^2 V = 0$$

Using dimensionless variables Laplace's equation is,

$$\frac{\partial^2 \theta}{\partial \rho^2} + \frac{1}{\rho}\frac{\partial \theta}{\partial \rho} + \frac{\partial^2 \theta}{\partial u^2} = 0 \tag{A-4}$$

Using separation of variables,

$$\theta = PE \tag{A-5}$$

Substituting equations (A-5) into (A-4):

$$\frac{P''}{P} + \frac{1}{\rho}\frac{P'}{P} + \frac{E''}{E} = 0$$

Therefore,

$$\frac{E''}{E} = -\alpha^2 \tag{A-6}$$

And,

$$P'' + \frac{1}{\rho} P' - \alpha^2 P = 0 \tag{A-7}$$

Solving equation (A-6),

$$E = C_1 \mathrm{Sin}(\alpha u) + C_2 \mathrm{Cos}(\alpha u) \tag{A-8}$$

Solving equation (A-7) the solution is in the form of Modified Bessel Functions:

$$P = C_3 I_0(\alpha \rho) + C_4 K_0(\alpha \rho) \tag{A-9}$$

Substituting equations (A-8) and (A-9) into (A-5):

$$\theta = \left[C_3 I_0(\alpha \rho) + C_4 K_0(\alpha \rho) \right] \left[C_1 \mathrm{Sin}(\alpha u) + C_2 \mathrm{Cos}(\alpha u) \right] \tag{A-10}$$

Applying the last boundary condition to (A-10):

$$a = \rho = b \qquad u = 1 \qquad \theta = 0$$

Then,

$$C_2 = 0 \qquad \mathrm{Sin}\,\alpha = 0 \quad \text{and} \quad \alpha = n\pi$$

Where, $n = 0, 1, 2, \ldots$ thus, equation (A-10) becomes:

$$\theta = C_0 + \sum_{n=1}^{\infty} \left[C_n I_0(n\pi\rho) + D_n K_0(n\pi\rho) \right] \mathrm{Sin}(n\pi u) \tag{A-11}$$

Using the other boundary conditions from equations (A-3):

$$a \le \rho \le b \qquad u = 0 \qquad \theta = 1$$

$$a = \rho = b \qquad u = 1 \qquad \theta = 0$$

Then,

$$C_0 = 1-u$$

And,

$$\theta = 1-u+\sum_{n=1}^{\infty}\left[C_nI_0(n\pi\rho)+D_nK_0(n\pi\rho)\right]\sin(n\pi u) \quad \text{(A-12)}$$

At the inner diameter of the annulus, using equation (A-12) the equation for the inner perimeter surface temperature is:

$$g(u) = (1-u)+\sum_{n=1}^{\infty}\left[C_nI_0(n\pi a)+D_nK_0(n\pi a)\right]\sin(n\pi u) \quad \text{(A-13)}$$

Correspondingly at the outer diameter of the annulus using equation (A-12) the equation of the outer perimeter surface is:

$$h(u) = (1-u)+\sum_{n=1}^{\infty}\left[C_nI_0(n\pi b)+D_nK_o(n\pi b)\right]\sin(n\pi u) \quad \text{(A-14)}$$

Letting,

$$a_n = C_nI_0\,(n\pi a) + D_nK_0\,(n\pi a) \quad \text{(A-15)}$$

$$b_n = C_nI_0\,(n\pi b) + D_nK_0\,(n\pi b) \quad \text{(A-16)}$$

Solving C_n and D_n from equations (A-15) and (A-16):

$$C_n = \frac{\begin{vmatrix} a_n & K_0\,(n\pi a) \\ b_n & K_0\,(n\pi b) \end{vmatrix}}{\begin{vmatrix} I_0\,(n\pi a) & K_0\,(n\pi a) \\ I_0\,(n\pi b) & K_0\,(n\pi b) \end{vmatrix}} \quad \text{(A-17)}$$

$$D_n = \frac{\begin{vmatrix} I_0(n\pi a) & a_n \\ I_0(n\pi b) & b_n \end{vmatrix}}{\begin{vmatrix} I_0(n\pi a) & K_0(n\pi a) \\ I_0(n\pi b) & K_0(n\pi b) \end{vmatrix}} \tag{A-18}$$

Substituting equations (A-15) into (A-13) and (A-16) into (A-14) and arranging so that:

$$u-1+g(u) = \sum_{n=1}^{\infty} a_n \mathrm{Sin}(n\pi u) \tag{A-19}$$

$$u-1+h(u) = \sum_{n=1}^{\infty} b_n \mathrm{Sin}(n\pi u) \tag{A-20}$$

Solving for the Euler coefficients a_n and b_n, it is necessary to use Euler-Fourier formulas.[1]

The half-range sine expansion is based upon extending $(u-1)+g(u)$ and $(u-1)+h(u)$ over the interval u of (-1,0) by reflection in the origin.

1: Drawing

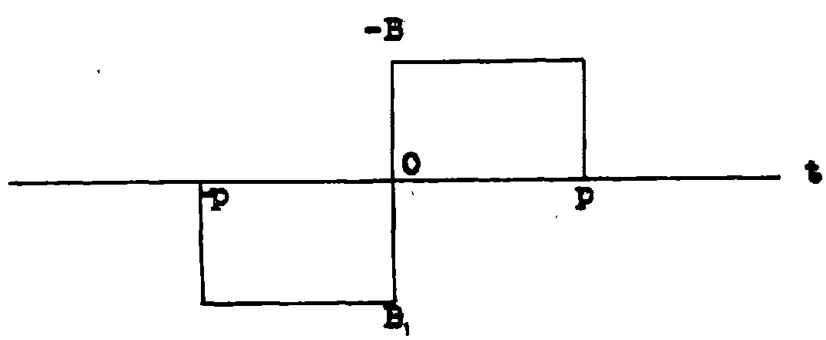

If BB_1 is chosen as the vertical axis, the graph defines an odd function by the theorem only sine terms

If,

$p = 1$ and $u = t$ (from footnote 1)

a_n and b_n are:

$$a_n = 2\int_0^1 \left[(u-1)+g(u)\right] \operatorname{Sin}(n\pi u)du \qquad \text{(A-21)}$$

$$b_n = 2\int_0^1 \left[(u-1)+h(u)\right] \operatorname{Sin}(n\pi u)du \qquad \text{(A-22)}$$

Using the boundary conditions for a linear guard:

$$H(Z)=V_1-(V_1-V_2)\frac{Z}{W} \qquad \text{(A-23)}$$

Substituting into equation (A-23) the dimensionless variables of the equation (A-2) and the boundary condition h(u) of equations (A-3):

$$h(u) = \frac{V_1-(V_1-V_2)u-V_2}{V_1-V_2}$$

Thus,

$$h(u) = 1-u \qquad \text{(A-24)}$$

By substituting equation (A-24) into (A-22):

$$b_n = 0 \qquad \text{(A-25)}$$

---

will appear in its expansion.
Theorem: If f(t) is an odd periodic function, then the coefficients in the Fourier series f(t) are given by the formulas:

$$A_n = 0 \qquad B_n = \frac{2}{p}\int_0^p f(t)\operatorname{Sin}\left(\frac{n\pi t}{p}\right)dt$$

The oddness depends upon the relation to the vertical axis of the coordinate system which can be arbitrarily chosen.

Differentiating equation (A-12):

$$\frac{d\theta}{d\rho} = \sum_{n=1}^{\infty} n\pi \mathrm{Sin}(n\pi u) \left[C_n I_0'(n\pi\rho) + D_n K_0'(n\pi\rho) \right]$$

$$\frac{d\theta}{d\rho} = \sum_{n=1}^{\infty} n\pi \mathrm{Sin}(n\pi u) \left[C_n I_1(n\pi\rho) - D_n K_1(n\pi\rho) \right] \qquad \text{(A-26)}$$

Let equation (A-26) define the surface of the annulus at the inner diameter A.

Substituting equations (A-17),(A-18),(A-25) into (A-26) the resulting equation for the inner diameter is:

$$\frac{\partial\theta}{\partial\rho} = \sum_{n=1}^{\infty} a_n n\pi \mathrm{Sin}(n\pi u) \left[\frac{K_0(n\pi b) I_1(n\pi a) + I_0(n\pi b) K_1(n\pi a)}{K_0(n\pi b) I_0(n\pi a) - I_0(n\pi b) K_0(n\pi a)} \right] \qquad \text{(A-27)}$$

The radial heat flow at the inner surface of the annulus, r = A, through a cylindrical surface element of length dZ is:

$$dp = 2\pi A \, K_i \left(\frac{\partial V}{\partial r} \right)_{r=A} dZ \qquad \text{(A-28)}$$

Using the dimensionless variables from the equations (A-2), equation (A-28) becomes:

$$dp = 2\pi a \sigma_i \left(\frac{\partial \theta}{\partial \rho} \right)_{\rho=a} du \qquad \text{(A-29)}$$

The total dimensionless radial heat flow across the inner cylindrical surface of the annulus is found by integrating equation (A-29) for limits between $u = u_1$ to $u = u_2$ which are defined in the analysis subsequently,

$$p(u)_1^2 = 2\pi a \sigma_i \int_{u_1}^{u_2} \left.\frac{\partial\theta}{\partial\rho}\right|_{\rho=a} du \tag{A-30}$$

Substituting equation (A-27) into (A-30) and integrating

$$p(u)_1^2 = \sum_{n=1}^{\infty} 2\pi a \sigma_i a_n \left[\mathrm{Cos}(n\pi u_1) - \mathrm{Cos}(n\pi u_2)\right] \left[\frac{K_0(n\pi b)I_1(n\pi a) + I_0(n\pi b)K_1(n\pi a)}{K_0(n\pi b)I_0(n\pi a) - I_0(n\pi b)K_0(n\pi a)}\right] \tag{A-31}$$

It is necessary to define a temperature distribution along the inner surface of the annulus, which then defines a_n.

Referring to Figure A-1: V_1 is the temperature at the matched end where $Z = 0$; S_s is the constant longitudinal temperature gradient in the specimen bar; and S_m is the constant longitudinal temperature gradient in the meter-bar.

The boundary conditions of the cut-bar define the temperature distribution along the inner surface of the annulus. This temperature is constant around the perimeter which is equal distant from the ends.

$0 \leq Z \leq M \qquad V = T - S_m Z$

$M \leq Z \leq M+L \qquad V = T - S_m M - S_s(Z-M)$

$m + L \leq Z \leq W \qquad V = T - S_m M - S_s L - S_m(Z-M-L) = S_m(W-Z)$

(A-32)

Using the dimensionless variables of equations (A-2) the above boundary conditions (A-32) are redefined for a dimensionless temperature distribution g(u):

$0 \leq u \leq m \qquad \theta = 1 - \Psi_m u$

$m \leq u \leq m + \ell \qquad \theta = 1 - \Psi_m m - \Psi_s(u-m)$

$m + \ell \leq u \leq 1 \qquad \theta = \Psi_m(1-u) \qquad \text{(A-33)}$

Where,

$$\Psi_m = \frac{S_m W}{T}, \quad \Psi_s = \frac{S_s W}{T} \qquad \text{(A-34)}$$

Using the above boundary conditions (A-33) and equation (A-21) the value for a_n can be defined as:

$$a_n = a_{n1} + a_{n2} + a_{n3} \qquad \text{(A-35)}$$

$$a_{n1} = 2\int_0^m u(1 - \Psi_m)\text{Sin}(n\pi u)du$$

$$a_{n1} = \frac{2(1-\Psi_m)}{n^2\pi^2}\left[\text{Sin}(n\pi m) - n\pi m\text{Cos}(n\pi m)\right] \qquad \text{(A-36)}$$

$$a_{n2} = 2\int_{m}^{m+\ell} (-\Psi_m m + \Psi_s m)\mathrm{Sin}(n\pi u)du$$

$$+2\int_{m}^{m+\ell} (1-\Psi_s)u\mathrm{Sin}(n\pi u)du$$

$$a_{n2} = \frac{2m(\Psi_s - \Psi_m)}{n\pi}\left[\mathrm{Cos}(n\pi m) - \mathrm{Cos}\,n\pi\,(m-\ell)\right]$$

$$+ \frac{2(1-\Psi_s)}{n^2\pi^2}\left[\mathrm{Sin}(n\pi m + n\pi\ell) - n\pi(m+\ell)\mathrm{Cos}\,(n\pi m + n\pi\ell)\right.$$

$$\left. - \mathrm{Sin}(n\pi m) + n\pi m\mathrm{Cos}(n\pi m)\right] \qquad \text{(A-37)}$$

$$a_{n3} = 2\int_{m+\ell}^{1}\left[\Psi_m - 1 + u(1-\Psi_m)\right]\mathrm{Sin}(n\pi u)du$$

$$a_{n3} = \frac{2(\Psi_m - 1)}{n\pi}\left\{\mathrm{Cos}\left[n\pi\,(m+\ell)\right] - \mathrm{Cos}(n\pi)\right\}$$

$$+ \frac{2(1-\Psi_m)}{n^2\pi^2}\left[-n\pi\mathrm{Cos}(n\pi) - \mathrm{Sin}(n\pi m + n\pi\ell)\right.$$

$$\left. + n\pi(m+\ell)\quad\mathrm{Cos}(n\pi m + n\pi\ell)\right] \qquad \text{(A-38)}$$

Substitute equations (A-36), (A-37), (A-38) into (A-35) and by arranging and reducing the Euler coefficients become:

$$a_n = \frac{4}{n^2\pi^2}(\Psi m - \Psi s)\left[\mathrm{Sin}\frac{(n\pi\ell)}{2}\,\mathrm{Cos}(\frac{n\pi}{2})\right] \qquad \text{(A-39)}$$

From equations (A-2) of dimensionless variables,

$$\sigma_s = \frac{K_s}{K_m} \qquad \text{(A-40)}$$

Assuming that there is no heat loss or gain in the cut-bar, it is possible to help reduce the mathematical analysis so that the resulting solution can be solved by computer with only a minor loss in the accuracy of the resulting data.

Thus,

$$K_m S_m = K_s S_s$$

Or,

$$\frac{S_m}{S_s} = \frac{K_s}{K_m} \qquad \text{(A-41)}$$

From equations (A-34), and (A-41) it can be shown that,

$$\frac{\Psi_s}{\Psi_m} = \frac{K_m}{K_s} \qquad \text{(A-42)}$$

Let Q represent the total Longitudinal heat flow through the cut-bar with the stipulation that there be no heat gained or lost through the surface between the cut-bar and the annulus.

Thus,

$$Q = \pi A^2 K_m S_m = \pi A^2 K_s S_s \qquad \text{(A-43)}$$

Defining heat flow Q in dimensionless parameters:

$$q = \frac{Q}{WTK_m} \qquad \text{(A-44)}$$

Using equations (A-34), (A-43) and (A-44), we have,

$$q = \pi a^2 \Psi_m \tag{A-45}$$

Defining the net fraction of power lost or gained in the annulus between $u = 0$ and $u = u_2$ as Ω. Heat loss in the cut-bar is the heat gained in the annulus; thus, the fractional power change γ in the cut-bar is,

$$\gamma = -\Omega = -\frac{p}{q} \tag{A-46}$$

Substituting in values for p, q into equation (A-46) by using equations (A-31), (A-39), (A-42), and (A-45):

$$\gamma = -K_1\left(\frac{1}{K_m} - \frac{1}{K_s}\right)\frac{8}{\pi^2 a} \sum_{n=1}^{\infty}\left[\frac{1-\text{Cos}(n\pi u_2)}{n^2}\right]$$

$$\left[\frac{K_0(n\pi b)I_1(n\pi a)+I_0(n\pi b)K_1(n\pi a)}{K_0(n\pi b)I_0(n\pi a)-I_0(n\pi b)K_0(n\pi a)}\right] \text{Sin}\left(\frac{n\pi \ell}{2}\right) \text{Cos}\left(\frac{n\pi}{2}\right) \tag{A-47}$$

Substituting the dimensionless variables of equation (A-2) into equation (A-47), equation (A-47) becomes:

$$\gamma = -K_1\left(\frac{1}{K_s} - \frac{1}{K_s}\right) \frac{8W}{\pi^2 A} \sum_{n=1}^{\infty}\left[\frac{1-\text{Cos}\left(\frac{n\pi Z}{W}\right)}{n^2}\right]$$

$$\left[\frac{K_0\left(\frac{n\pi B}{W}\right)I_1\left(\frac{n\pi A}{W}\right)+ I_0\left(\frac{n\pi B}{W}\right) K_1\left(\frac{n\pi A}{W}\right)}{K_0\left(\frac{n\pi B}{W}\right)I_0\left(\frac{n\pi A}{W}\right)- I_0\left(\frac{n\pi B}{W}\right) K_0\left(\frac{n\pi A}{W}\right)}\right] \text{Sin}\left(\frac{n\pi L}{2W}\right) \text{Cos}\left(\frac{n\pi}{2}\right) \tag{A-48}$$

γ is the per cent heat loss relative to the total heat flow in the cut-bar assuming that the total heat flow is the flow when there would be no loss or gain in the flow from or to the powder insulation annulus,

γ is called the fractional power change.

Letting,

$$\gamma = F_k F_g \tag{A-49}$$

Where,

$$F_k = K_i\left(\frac{1}{K_m} - \frac{1}{K_s}\right) \tag{A-50}$$

F_k is the thermal conductivity factor of the fractional power change,

And,

$$F_g = \frac{8W}{\pi^2 A}\sum_{n=1}^{\infty}\left[\frac{1-\text{Cos}\left(\frac{n\pi Z}{W}\right)}{n^2}\right]$$

$$\left[\frac{K_0\left(\frac{n\pi B}{W}\right)I_1\left(\frac{n\pi A}{W}\right) + I_0\left(\frac{n\pi B}{W}\right)K_1\left(\frac{n\pi A}{W}\right)}{K_0\left(\frac{n\pi B}{W}\right)I_0\left(\frac{n\pi A}{W}\right) - I_0\left(\frac{n\pi B}{W}\right)K_0\left(\frac{n\pi A}{W}\right)}\right]\text{Sin}\left(\frac{n\pi L}{2W}\right)\text{Cos}\left(\frac{n\pi}{2}\right) \tag{A-51}$$

It is necessary to simplify equation (A-51) for computer analysis since,

$$\text{Cos}\left(\frac{n\pi}{2}\right) = 0 \text{ when n is odd}$$

Therefore,

$$(-1)^{\frac{n}{2}} = \mathrm{Cos}\left(\frac{n\pi}{2}\right) \text{ when n is even} \qquad \text{(A-52)}$$

Letting, $m = \frac{n}{2}$ (A-53)

Substituting equations (A-53), (A-52) into equation (A-51), the index of equation (A-51) can be changed with no loss to the equation.

Therefore,

$$F_g = \frac{2W}{\pi^2 A} \sum_{m=1,2,\ldots}^{\infty} (-1)^m \left[\frac{1-\mathrm{Cos}\frac{2\pi Z m}{W}}{m^2}\right]$$

$$\left[\frac{K_0\left(\frac{2m\pi B}{W}\right) I_1\left(\frac{2m\pi A}{W}\right) + I_0\left(\frac{2m\pi B}{W}\right) K_1\left(\frac{2m\pi A}{W}\right)}{K_0\left(\frac{2m\pi B}{W}\right) I_0\left(\frac{2m\pi A}{W}\right) - I_0\left(\frac{2m\pi B}{W}\right) K_0\left(\frac{2m\pi A}{W}\right)}\right] \mathrm{Sin}\left(\frac{m\pi L}{W}\right) \qquad \text{(A-54)}$$

F_g is the geometrical factor of the fractional change.

APPENDIX B

COMPUTER PROGRAM OF GEOMETRICAL FACTOR

A computer program was developed to calculate the large number of data points needed to plot the design charts. Also, this program was utilized in the error analysis of any particular apparatus. A particular range of design dimensions can be identified by the use of these charts. The exact error for a given set of dimensions can be found by using the program.

In Appendix A, the resulting solution is described in a mathematical equation (A-54) for the geometrical factor of the cut-bar apparatus. This equation is reproduced below:

$$F_g = \frac{2W}{\pi^2 A} \sum_{m=1,2,..}^{\infty} (-1)^m \left[\frac{1-\mathrm{Cos}\left(\frac{2\pi m Z}{W}\right)}{m^2}\right]$$

$$\left[\frac{K_0\left(\frac{2m\pi B}{W}\right) I_1\left(\frac{2m\pi A}{W}\right) + I_0\left(\frac{2m\pi B}{W}\right) K_1\left(\frac{2m\pi A}{W}\right)}{K_0\left(\frac{2m\pi B}{W}\right) I_0\left(\frac{2m\pi A}{W}\right) - I_0\left(\frac{2m\pi B}{W}\right) K_0\left(\frac{2m\pi A}{W}\right)}\right] \mathrm{Sin}\left(\frac{m\pi L}{W}\right) \tag{B-1}$$

Two computer programming approaches are obvious. The first approach uses a large memory bank where all of the Modified Bessel Function of the first and second kind, and of the first and second order, are stored. Using this method, it is necessary to use approximation techniques to find the Modified Bessel Functions of fractional arguments. This method can be used only in a data reduction center having the necessary facilities. The second approach is to generate the Modified Bessel Function in a program when needed.

The second approach was used in this thesis because the IBM 1620 Computer which was available was limited in size and speed, and the computer program using the Fortran language was efficient. The program can function in the Fortran II, Fortran IV, or Forgo language, and with a small change it can function in PDQ language.

Inputs into the following programs are: W, A, B, CL, TEST, JA, MM, LP.

W - length of the annulus.

A - the diameter of the specimen bar and meterbar, or the inner diameter of the annulus.

B - the outer diameter of the annulus or the inner diameter of the cylindrical guard.

CL- the longitudinal length of the specimen bar. It is represented by L in the equation (B-1).

TEST- the accuracy of the resulting output F_g. TEST stops the program or truncates the series when it has converged so the F_g is varying within the range of the TEST input.

JA - the number of points for which F_g output is formed along one-half of the bar. It is the number of Z points into which one-half of the bar is dividided.

MM - the limiting number of terms in the series. It represents the maximum number of terms at which the series or program will be truncated. At some points, the series will converge only at a very large number of terms.

LP - the frequency of the test for convergence of the series. It must be an odd number and it is based on the $\frac{2W}{L}$. With familiarity in using the program, an engineer's intuitiveness can find a reasonable LP.

Figure B-1 illustrates the flow-chart for the computer program. Three computer programs were developed based on this flow-chart and the available facilities. The computer program illustrated in Figure B-2 was developed for use on an IBM-1620 computer. Using this program as a source deck, an objective deck can be compiled in Fortran II and PDQ. This program can be used directly in Forgo language. Figure B-3 illustrates a computer program which can be used on a time-sharing-computer system, using Fortran IV language, and this program can be modified with the addition of the program statement lines illustrated in Figure B-4. This modification expands the program so that a large amount of data can be handled.

FIGURE B-1

COMPUTER PROGRAM FLOW-CHART

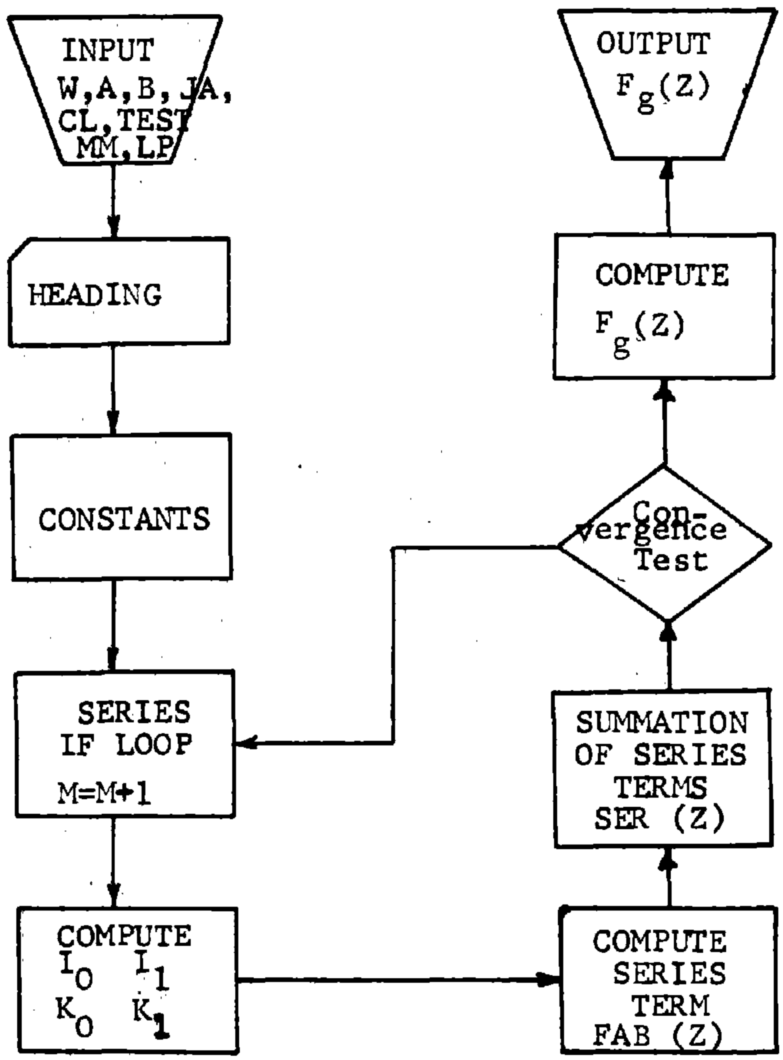

<u>FIGURE B-2</u>

COMPUTER PROGRAM FOR IBM-1620 COMPUTER

```
    DIMENSION FAB(20),FB(20),Z(20),FG(20),SER(20),
    BST(20),KL(20)
    PI=3.1415927
    GAM=.57721566
    PUNCH 910
10  READ 905,W,A,B,CL,TEST,JA,MM,LP
    PUNCH 920,JA
    PUNCH 930
    PUNCH 935,W,A,B,CL,TEST,JA,MM,LP
    SIGN = 1.
    EP = 1.
    DOG = 1.
    ENT = EXPF((-4.*(B-A)*PI)/W)
    H = (2.0*W)/(PI*PI*A)
    CAT = JA
    DO 20 N= 1,JA
    ZA = N
    Z (N) = ZA*W/(2.*CAT)
    SER(N)=0.0
    BST(N)=9999.
    KL(N)=0
20  FAB(N)=1.0
    M=0
```

```
 30   M=M+1
      DOG=DOG*ENT
      V=M
      XV=2.*V*PI/W
      RRI=V*PI/CAT
      SIGN= -SIGN
      Y=SINF(V*PI*CL/W)*SIGN/(V*V)
      X=A*XV
      CKS=X
      KK=0
 40   NORD=0
500   BK=0.0
      FN=NORD
      IF(X-FN-6.)501,700,700
501   XA=X/2.
      XB=XA*XA
      N=0
503   AN=N
      T=1.
      S= -1.
510   IF(AN)9999,520,512
512   T=T*XA/AN
      AN=AN-1.
      GO TO 510
```

```
520   BIN=T
      DO 530 K=1,9999
      DEN=K*(K+N)
      T=T*XB/DEN
      IF((BIN+T)-BIN)525,550,525
525   BIN=BIN+T
530   CONTINUE
550   IF(N-1)575,630,555
555   IF(X-FN-3.)1111,1111,700
565   N=1
      BIO=BIN
      BKO=BK
      GO TO 503
575   BK= -(GAM+LOGF(XA))*BIN
      T=XB
      S=1.
      XI=1.
      DO 610 K=2,9999
      AK=K
      IF((BK+T*XI)-BK)600,620,600
600   BK=BK+T*XI
      T=T*XB/(AK*AK)
      XI=XI+1./AK
610   CONTINUE
620   IF(NORD)9999,555,565
```

```
630   BK=(1./X-BIN*BKO)/BIO
      IF(NORD-1)9999,555,9999
700   C=4*NORD*NORD
      D=8.*X
      CON2=1./SQRTF(2.*PI*X)
      CON3=SQRTF(PI/(2.*X))
      AN=NORD
      PHI=X-(2.*AN+1.)/4.*PI
      K=X+1.+SQRTF(X*X+AN*AN)
      T=(C-1.)/D
      S=1.
      U=1.
      PN=1.
      QN=T
      BK=1.+T
      BI=1.-T
      DO 735 I=2,K
      AI=I
      T=(C-(2.*AI-1.)**2)/D*T/AI
      BK=BK+T
      BI=BI+T*S
      IF((BI+T)-BI)730,738,730
730   S= -S
735   CONTINUE
```

```
738  IF(CKS-7.)741,755,755
741  BK=EXPF(-X)*CON3*BK
     IF(X-FN-6.)1111,750,750
750  BIN=EXPF(X)*CON2*BI
     GO TO 1111
755  BK=CON3*BK
760  BIN=CON2*BI
     EP=DOG
1111 NORD=FN
     IF(NORD)9999,810,830
810  IF(KK)9999,820,840
820  GA=BIN
     GB=BK
     NORD=1
     GO TO 500
830  GC=BIN
     GD=BK
     X=XV*B
     KK=1
     GO TO 40
840  GE=BIN
     GF=BK*EP
     R=(GF*GC+GE*GD)/(GF*GA-GE*GB)
     FA=Y*R
```

```
      LPF=0
      DO 860 N=1,JA
      IF(KL(N)-3)845,850,858
 845  LPF=1
 850  ZA=N
      FB(N)=1.0-COSF(RRI*ZA)
      FAB(N)=FA*FB(N)
      SER(N)=SER(N)+FAB(N)
      IF(M/LP*LP-M)860,852,860
 852  IF(TEST-ABS(BST(N)-SER(N)))854,856,856
 854  KL(N)=0
      BST(N)=SER(N)
      GO TO 860
 856  BST(N)=SER(N)
 858  KL(N)=KL(N)+1
 860  CONTINUE
      IF(LPF-1)890,888,9999
 888  IF(M-MM)30,890,890
 890  PUNCH 960,M
      DO 900 J=1,JA
      FG(J)=H*SER(J)
 900  PUNCH 940,J,Z (J),KL(J),SER(J),FG(J)
      GO TO 10
9999  PUNCH 9998
      GO TO 10
 905  FORMAT (5F10.5,3I5)
```

```
 910  FORMAT (///12X,46HRESULTS OF POWER LOSS OVER
      LENGTH OF METER-BAR//)

 920  FORMAT (///12X,15HFG VERSUS Z FOR,I3,23H
      POINTS FROM Z=0 TO END//)

 930  FORMAT (6X.1HW,9X,1HA,9X,1HB,9X,1HL,8X,4HTEST,
      5X,1HP,3X,1HM,4X,1HF)

 935  FORMAT (5F10.5,3I5///)

 940  FORMAT (I10,F14.5,I8,3X,2F10.7)

 960  FORMAT (//7X,5HPOINT,8X,1HZ,9X,2HKL,7X,3HSER,
      8X,2HFG,5X,2HM=,I3)

9998  FORMAT (//25X,5HERROR//)

      END
```

FIGURE B-3

COMPUTER PROGRAM FOR TIME-SHARING COMPUTER

```
10   DIMENSION FAB(30),FB(30),Z(30),FG(30),SER(30),
     BST(30),KL(30)
20   PI=3.1415927
30   GAM=.57721566
40   PRINT 910
50   10 INPUT,W,A,B,CL,TEST,JA,MM,LP
60   PRINT 920,JA
70   PRINT 930
80   PRINT 935,W,A,B,CL,TEST,JA,MM,LP
85   SIGN=1.
90   EP=1.
100  DOG=1.
110  ENT=EXPF((-4.*(B-A)*PI)/W)
120  H=(2.0*W)/(PI*PI*A)
130  CAT=JA
140  DO 20 N=1,JA
150  ZA=N
160  Z(N)=ZA*W/(2.*CAT)
170  SER(N)=0.0
180  BST(N)=9999.
190  KL(N)=0
200  20 FAB(N)=1.0
```

```
M=0
30 M=M+1
DOG=DOG*ENT
V=M
XV=2.*V*PI/W
SIGN= -SIGN
Y=SINF(V*PI*CL/W)*SIGN/(V*V)
RRI=V*PI/CAT
X=A*XV
CKS=X
KK=0
40 NORD=0
500 BK=0.0
FN=NORD
IF(X-FN-6.)501,700,700
501 XA=X/2.
XB=XA*XA
N=0
503 AN=N
T=1.
S= -1.
510 IF(AN)9999,520,512
512 T=T*XA/AN
AN=AN-1.
GO TO 510
```

```
520 BIN=T
DO 530 K=1,9999
DEN=K*(K+N)
T=T*XB/DEN
IF((BIN+T)-BIN)525,530,525
525 BIN=BIN+T
530 CONTINUE
550 IF(N-1)575,630,555
555 IF(X-FN-3.)1111,1111,700
565 N=1
BIO=BIN
BKO=BK
GO TO 503
575 BK= -(GAM+LOGF(XA))*BIN
T=XB
S=1.
XI=1.
DO 610 K=2,9999
AK=K
IF((BK+T*XI)-BK)600,620,600
600 BK=BK+T*XI
T=T*XB/(AK*AK)
XI=XI+1./AK
610 CONTINUE
620 IF(NORD)9999,555,565
```

```
630 BK=(1./X-BIN*BKO)/BIO
IF(NORD-1)9999,555,9999
700 C=4*NORD*NORD
D=8.*X
CON2=1./SQRTF(2.*PI*X)
CON3=SQRTF(PI/(2.*X))
AN=NORD
PHI=X-(2.*AN+1.)/4.*PI
K=X+1.+SQRTF(X*X+AN*AN)
T=(C-1.)/D
S=1.
U=1.
PN=1.
QN=T
BK=1.+T
BI=1.-T
DO 735 I=2,K
AI=I
T=(C-(2.*AI-1.)**2)/D*T/AI
BK=BK+T
BI=BI+T*S
IF((BI+T)-BI)730,738,730
730 S= -S
735 CONTINUE
```

```
738 IF(CKS-7.)741,755,755
741 BK=EXPF(-X)*CON3*BK
IF(X-FN-6.)1111,750,750
750 BIN=EXPF(X)*CON2*BI
GO TO 1111
755 BK=CON3*BK
760 BIN=CON2*BI
EP=DOG
1111 NORD=FN
IF(NORD)9999,810,830
810 IF(KK)9999,820,840
820 GA=BIN
GB=BK
NORD=1
GO TO 500
830 GC=BIN
GD=BK
X=XV*B
KK=1
GO TO 40
840 GE=BIN
GF=BK*EP
R=(GF*GC+GE*GD)/(GF*GA-GE*GB)
FA=Y*R
```

```
LPF=0
DO 860 N=1,JA
IF(KL(N)-3)845,850,858
845 LPF=1
850 ZA=N
FB(N)=1.0-COSF(RRI*ZA)
FAB(N)=FA*FB(N)
SER(N)=SER(N)+FAB(N)
IF(M/LP*LP-M)860,852,860
852 IF(TEST-ABS(BST(N)-SER(N)))854,856,856
854 KL(N)=0
BST(N)=SER(N)
GO TO 860
856 BST(N)=SER(N)
858 KL(N)=KL(N)+1
860 CONTINUE
IF(LPF-1)890,888,9999
888 IF(M-MM)30,890,890
890 PRINT 960,M
DO 900 J=1,JA
FG(J)=H*SER(J)
900 PRINT 940,J,Z (J),KL(J),SER(J),FG(J)
GO TO 10
9999 PRINT 9998
```

```
GO TO 10
910 FORMAT (//12X,46HRESULTS OF POWER LOSS
OVER LENGTH OF METER-BAR//)
920 FORMAT (///12X,15HFG VERSUS Z FOR, I3,
23H POINTS FROM Z=O TO END//)
930 FORMAT (6X,1HW,9X,1HA,9X,1HB,9X,1HL,8X,
4HTEST,5X,1HP,3X,1HM,4X,1HF)
935 FORMAT (5F10.5,3I5///)
940 FORMAT (I10,F14.5,I8,3X,2F10.7)
960 FORMAT (//7X,5HPOINT,8X,1HZ,9X,2HKL,7X,
3HSER,8X,2HFG,5X,2HM=,I3)
9998 FORMAT (//25X,5HERROR//)
END
```

FIGURE B-4

COMPUTER PROGRAM FOR TIME-SHARING COMPUTER

```
50    10 READ,W,A,B,CL,TEST,JA,MM,LP
746   $DATA
```

TECHNICAL REPORTS DISTRIBUTION LIST, CONTRACT NOnr 2249(12)

Office of Naval Research (5)
Department of the Navy
Washington, D. C. 20360
ATTN: Code 429

Naval Ship Engineering Center (5)
Department of the Navy
Washington, D. C. 20360
ATTN: Library (2), Code 6645 (3)

Naval Air Systems Command (5)
Department of the Navy
Washington, D. C. 20360
ATTN: Library

Director
Naval Research Laboratory (7)
Washington 25, D. C.
ATTN: Technical Information Div.

Marine Engineering Laboratory
Annapolis, Maryland (2)

U. S. Naval Postgraduate School (2)
Monterey, California
ATTN: Library

Office of the Asst. (1)
Chief of Staff, G-4
Research and Development Div.
Department of the Army
Washington, D. C. 20360

Defense Documentation Center (20)
Cameron Station
Alexandria, Virginia

U. S. Army (1)
Ordnance Missile Command
Army Ballistic Missile Agency
Redstone Arsenal, Alabama
ATTN: ORDAB-RRT

U. S. Atomic Energy Commission (2)
Technical Information Service
P. O. Box 62
Oak Ridge, Tennessee

Director (1)
Engineering Res. and Dev. Lab
Fort Belvoir, Virginia
ATTN: Head, Nuclear Power Branch

U. S. Coast Guard Hq. (1)
Testing and Development Div.
1300 "E" Street
Washington, D. C.

National Aeronautics and (1)
Space Administration
Ames Research Center
Moffett Field, California
ATTN: Library

National Aeronautics and (1)
Space Administration
Langley Research Center
Langley Field
Hampton, Virginia
ATTN: Library

National Aeronautics and (2)
Space Administration
Lewis Research Center
21000 Brookpark Road
Cleveland 35, Ohio
ATTN: Library

The Babcock and Wilcox Co. (1)
Research and Dev. Center
P. O. Box 835
Alliance, Ohio

Battelle Memorial Institute (1)
505 King Avenue
Columbus 1, Ohio

Brookhaven National Laboratory (1)
Technical Information Division
Upton, Long Island, New York
ATTN: Research Library

Electric Boat Company (2)
Groton, Connecticut
ATTN: Mr. E. S. Dennison

TECHNICAL REPORTS DISTRIBUTION LIST, CONTRACT NOnr 2249(12) (Cont'd)

Carrier Corporation (1)
300 South Geddes Street
Syracuse 1, New York
ATTN: Engineering Library

General Motors Corp. (2)
Allison Division
Indianapolis 6, Indiana
ATTN: Mr. R. M. Hazen,
Dir. of Engrg.

General Motors Corp (2)
Research Laboratories
12 Mile and Mound Roads
Warren, Michigan

California Inst. of Technology (1)
Mechanical Engineering Dept.
1201 East California Street
Pasadena 4, California
ATTN: Mechanical Engrg. Library

University of California (1)
College of Engineering
Berkeley 4, California

University of California at (1)
Los Angeles
Engineering Department
Los Angeles 24, California

The Catholic University of America (1)
Department of Mechanical Engineering
Washington 17, D. C.

Columbia University (1)
Heat Transfer Research Facility
P. O. Box 245, Station J
New York 27, New York

Cornell University (1)
College of Engineering
Dept. of Heat Power Engrg.
Ithaca, New York

University of Houston (1)
Mechanical Engineering Dept.
Houston, Texas

Illinois Inst. of Technology (1)
Dept. of Mechanical Engrg.
Technology Center
Chicago 16, Illinois
ATTN: Heat Transfer Lab

University of Illinois (1)
Mechanical Engineering Department
Urbana, Illinois

Massachusetts Inst. of Tech. (1)
Cambridge 39, Massachusetts
ATTN: Prof. William H. McAdams

University of Michigan (1)
228 W. Engineering Bldg.
Ann Arbor, Michigan

University of Minnesota (1)
Mechanical Engineering Dept.
Minneapolis, Minnesota
ATTN: Dr. E. R. G. Eckert

General Electric Company (2)
Small Aircraft Engine Dept.
1000 Western Ave.
West Lynn 3, Massachusetts
ATTN: Marine Indistrial Market
Development
(Internal Distribution by Company)

General Electric Company (2)
Cincinnati 15, Ohio
ATTN: Mr. M. E. Lapides,
Aircraft
Nuclear Propulsion Department

General Electric Company (2)
General Engineering Lab
Schenectady 5, New York
(Internal Distribution by Company)

Lockheed Aircraft Corp. (2)
Missile Systems Division
Aerodynamics Dept.
Sunnyvale, California
ATTN: Mr. G. A. Etemad

Ford Motor Company (1)
Dearborne, Michigan
ATTN: Mrs. Rachel MacDonald
Eng. Staff Library

The Franklin Institute (1)
Laboratories for Research and Dev.
Philadelphia 3, Pa.
ATTN: Mr. F. L. Jackson

General Dynamics Corp. (2)
General Atomic Division
P. O. Box 608
San Diego 12, California

Westinghouse Electric Corp. (2)
Lester Branch P. O.
Philadelphia 13, Pennsylvania
ATTN: Mr. F. K. Fischer, Mgr.
Dev. Engrg.

Modine Manufacturing Co. (2)
1500 DeKoven Avenue
Racine, Wisconsin
ATTN: Mr. C. T. Perkins, Pres.

Morgantown Research Center (1)
Bureau of Mines
Morgantown, West Virginia
ATTN: Mr. J. McGee

North American Aviation, Inc. (1)
International Airport
Los Angeles 45, California

United Aircraft Corp. (2)
400 Main Street
East Hartford 8, Conn.
ATTN: Mr. Robert C. Sale
Chief Librarian

The Trane Company (2)
2nd and Cameron Avenue
La Crosse, Wisconsin

Solar Aircraft Company (1)
San Diego 12, California
ATTN: Mr. P. A. Pitt,
Chief Engineer

Worthington Corp. (2)
Harrison Division
Harrison, New Jersey
ATTN: Mr. Normal L. Myerson,
Director of Research

Young Radiator Company (2)
703 S. Marquette Street
Racine, Wisconsin
ATTN: Mr. H. P. Brinen,
Res. Engineer

Unclassified
Security Classification

DOCUMENT CONTROL DATA - R&D

(Security classification of title, body of abstract and indexing annotation must be entered when the overall report is classified)

1. ORIGINATING ACTIVITY (Corporate author) The Catholic University of America Department of Mechanical Engineering Washington, D. C. 20017	2a. REPORT SECURITY CLASSIFICATION Unclassified 2b. GROUP

3. REPORT TITLE
An Analysis and Design of a Linear Guarded Cut-Bar Apparatus for Thermal Conductivity Measurements

4. DESCRIPTIVE NOTES (Type of report and inclusive dates)
Technical Report

5. AUTHOR(S) (Last name, first name, initial)
David A. Didion

6. REPORT DATE	7a. TOTAL NO. OF PAGES	7b. NO. OF REFS
31 Jan 1968	71	3

8a. CONTRACT OR GRANT NO. NOnr 2249(12) b. PROJECT NO. c. d.	9a. ORIGINATOR'S REPORT NUMBER(S) Technical Report No. 2 9b. OTHER REPORT NO(S) (Any other numbers that may be assigned this report)

10. AVAILABILITY/LIMITATION NOTICES
Qualified Requesters may obtain copies of this report from D.D.C.

11. SUPPLEMENTARY NOTES	12. SPONSORING MILITARY ACTIVITY Office of Naval Research Power Branch (Code 429) Washington, D. C. 20390

13. ABSTRACT

A quantitative analysis of the Cut-Bar method of measuring the thermal conductivity of solids is performed. The mathematical model, which corrects for the difference in heat flux in the specimen and reference standard, is that of the two dimensional steady heat conduction equation applied to an annulus of insulation. The solution is presented in detail and found to be comprised of two physically distinct parts, a conductivity factor and a geometrical factor. A number of charts and graphs are presented for clarification as to the nature and magnitude the relative sizes of the various components will have on the accuracy over different conductivity ranges. The complexity of the geometrical factor required a digital computer programs which are included.

Reference is made to a similar study, performed by researchers at the National Bureau of Standards. It is found that the differences in the guard temperature distribution results in a substantial change in the geometrical factor. ( )

Unclassified

Security Classification

14. KEY WORDS	LINK A		LINK B		LINK C	
	ROLE	WT	ROLE	WT	ROLE	WT
Thermal Conductivity Measurements Heat Conduction						

INSTRUCTIONS

1. ORIGINATING ACTIVITY: Enter the name and address of the contractor, subcontractor, grantee, Department of Defense activity or other organization *(corporate author)* issuing the report.

2*a*. REPORT SECURITY CLASSIFICATION: Enter the overall security classification of the report. Indicate whether "Restricted Data" is included. Marking is to be in accordance with appropriate security regulations.

2*b*. GROUP: Automatic downgrading is specified in DoD Directive 5200.10 and Armed Forces Industrial Manual. Enter the group number. Also, when applicable, show that optional markings have been used for Group 3 and Group 4 as authorized.

3. REPORT TITLE: Enter the complete report title in all capital letters. Titles in all cases should be unclassified. If a meaningful title cannot be selected without classification, show title classification in all capitals in parenthesis immediately following the title.

4. DESCRIPTIVE NOTES: If appropriate, enter the type of report, e.g., interim, progress, summary, annual, or final. Give the inclusive dates when a specific reporting period is covered.

5. AUTHOR(S): Enter the name(s) of author(s) as shown on or in the report. Enter last name, first name, middle initial. If military, show rank and branch of service. The name of the principal author is an absolute minimum requirement.

6. REPORT DATE: Enter the date of the report as day, month, year; or month, year. If more than one date appears on the report, use date of publication.

7*a*. TOTAL NUMBER OF PAGES: The total page count should follow normal pagination procedures, i.e., enter the number of pages containing information.

7*b*. NUMBER OF REFERENCES: Enter the total number of references cited in the report.

8*a*. CONTRACT OR GRANT NUMBER: If appropriate, enter the applicable number of the contract or grant under which the report was written.

8*b*, 8*c*, & 8*d*. PROJECT NUMBER: Enter the appropriate military department identification, such as project number, subproject number, system numbers, task number, etc.

9*a*. ORIGINATOR'S REPORT NUMBER(S): Enter the official report number by which the document will be identified and controlled by the originating activity. This number must be unique to this report.

9*b*. OTHER REPORT NUMBER(S): If the report has been assigned any other report numbers *(either by the originator or by the sponsor)*, also enter this number(s).

10. AVAILABILITY/LIMITATION NOTICES: Enter any limitations on further dissemination of the report, other than those imposed by security classification, using standard statements such as:

(1) "Qualified requesters may obtain copies of this report from DDC."

(2) "Foreign announcement and dissemination of this report by DDC is not authorized."

(3) "U. S. Government agencies may obtain copies of this report directly from DDC. Other qualified DDC users shall request through
____________________________________."

(4) "U. S. military agencies may obtain copies of this report directly from DDC. Other qualified users shall request through
____________________________________."

(5) "All distribution of this report is controlled. Qualified DDC users shall request through
____________________________________."

If the report has been furnished to the Office of Technical Services, Department of Commerce, for sale to the public, indicate this fact and enter the price, if known.

11. SUPPLEMENTARY NOTES: Use for additional explanatory notes.

12. SPONSORING MILITARY ACTIVITY: Enter the name of the departmental project office or laboratory sponsoring *(paying for)* the research and development. Include address.

13. ABSTRACT: Enter an abstract giving a brief and factual summary of the document indicative of the report, even though it may also appear elsewhere in the body of the technical report. If additional space is required, a continuation sheet shall be attached.

It is highly desirable that the abstract of classified reports be unclassified. Each paragraph of the abstract shall end with an indication of the military security classification of the information in the paragraph, represented as *(TS)*, *(S)*, *(C)*, or *(U)*.

There is no limitation on the length of the abstract. However, the suggested length is from 150 to 225 words.

14. KEY WORDS: Key words are technically meaningful terms or short phrases that characterize a report and may be used as index entries for cataloging the report. Key words must be selected so that no security classification is required. Identifiers, such as equipment model designation, trade name, military project code name, geographic location, may be used as key words but will be followed by an indication of technical context. The assignment of links, roles, and weights is optional.